

ARTICLE

Received 00th January 20xx,
Accepted 00th January 20xx

DOI: 10.1039/x0xx00000x

Designing Bijels formed by Solvent Transfer Induced Phase Separation with Functional Nanoparticles

Stephen Boakye-Ansah,^{*a} Matthew S. Schwenger^a and Martin F. Haase^a

Bicontinuous interfacially jammed emulsion gels (bijels) formed via solvent transfer induced phase separation (STriPS) are new soft materials with potential applications in separations, healthcare, or catalysis. To facilitate their applications, means to fabricate STriPS bijels with nanoparticles of various surface chemistries are needed. Here, we investigate the formation of STriPS bijels with nanoparticles of different wettabilities, ranging from partially hydrophobic to extremely hydrophilic. To this end, the surface wettability of silica nanoparticles is tailored by functionalization with ligands bearing either hydrophobic or hydrophilic terminal groups. We show that partially hydrophobic particles with acrylate groups can impart short-term stability to STriPS bijels on their own. However, to enable long-term stability, the use of cationic surfactants is needed. Partially hydrophobic particles require short chain surfactants for morphological stability while glycerol-functionalized hydrophilic particles require double chain cationic surfactants. Variation of the surfactant concentration results in various STriPS bijel morphologies with controllable domain sizes. Last, we show that functional groups on the nanoparticles facilitate interfacial cross-linking for the purposes of reinforcing STriPS bijels. Our research lays the foundation for the use of a wide variety of solid particles, irrespective of their surface wettabilities, to fabricate bijels with potential applications in Pickering interfacial catalysis and as cross-flow microreactors.

1 Introduction

The discovery of bicontinuous interfacially jammed emulsion gels (bijels) provided a pathway for the synthesis of static interpenetrating biphasic liquid microstructures.^{1–3} These structures are stabilized at the interface by a percolating layer of colloidal particles. Bijel-derived materials present interesting features such as high surface area, high porosity, structural tunability, high particle loadings, and easy fabrication, which make them highly attractive for applications including sensor technologies,⁴ separation processes,⁵ tissue engineering,⁶ battery electrodes,⁷ and fuel cells.⁸ By transforming bijels into polymeric materials, researchers have derived useful materials such as hierarchical porous templates,⁹ electrode materials for

both supercapacitor and fuel cells,^{8,10,11} porous hydrogels for biomedical applications⁶ and multifunctional nanocomposite membranes for water purification.⁵

The formation of bijels typically involves the interfacial arrest of two immiscible liquids undergoing spinodal decomposition which are mechanically stabilized in a non-equilibrium configuration by a jammed monolayer of colloidal particles at their interface.^{1,2} As first experimentally demonstrated by Herzig et al., thermal quenching of binary liquid mixtures resulted in the formation of bijels characterized by large domain sizes ($\sim 40\mu\text{m}$).² By using smaller-sized particles ($< 100\text{nm}$), bijels with sub-micrometre domains have also been realized, contributing to the generation of bicontinuous morphologies with high surface areas.^{12–15}

Moreover, Composto and coworkers have also demonstrated the control of polymeric bicontinuous morphologies via the segregation and jamming of nanoparticles at the interphase of polymer blends undergoing phase separation.^{16,17} For example, the partitioning behaviour of polymer-grafted silica nanoparticles (SNPs) depended on both the chain length and the end group of the polymer-brush, which also determined the morphology of the nanocomposite material.¹⁷

^a Rowan University, Henry M. Rowan College of Engineering, Department of Chemical Engineering, 201 Mullica Hill Rd., Glassboro, NJ 08028 USA.
E-mail: haasem@rowan.edu

[†] M.F.H. and S.B.-A. designed the study, S.B.-A. carried out most of the experiments, M.S.S. measured the ternary phase equilibrium. M.F.H. and S.B.-A. wrote the manuscript.

^{††} Electronic Supplementary Information (ESI) available: [details of any supplementary information available should be included here]. See DOI: 10.1039/x0xx00000x

Solid particles used for bijel stabilization typically have spherical shapes,^{2,12,15,18} but rod-shaped particles,¹⁹ 2D graphene oxide sheets,²⁰ and microbial cells²¹ can also stabilize bijels. Incorporating nanoparticles into bicontinuous materials not only imparts functional properties, but also the type, shape, and surface properties of the particles can be used to control their morphology. An example is what Hayward *et al.* showed, that beside interfacial jamming of particles, colloidal gelation in one phase of a polymer blend could arrest bicontinuous structures.²² The shape of the particles (nanorods or nanospheres) affected the morphology,²² similar to what Clegg *et al.* observed for bijels formed by phase separation.¹⁹

Recently, new approaches to simplify the fabrication of bijels by circumventing the limitations of thermal quenching have been introduced. Haase *et al.* introduced Solvent Transfer Induced Phase Separation (STriPS) for the fabrication of hierarchical and asymmetric bijel fibers, particles and films.^{5,14,23} STriPS generates bijels out of a broad selection of immiscible liquid combinations, since a solvent is used to create the initial homogeneous mixture of the immiscible liquids undergoing phase separation.

The next dramatic step in simplifying bijel formation was taken independently from each other by Cai *et al.*, as well as Huang *et al.* They discovered that bijels can be formed by simply shaking up a mixture of two immiscible fluids with surface-active particles. These advances further broaden the selection of immiscible liquids deployable to form bijels. Cai *et al.* introduced a multistep homogenization procedure with fluids of increased viscosities.¹⁴ The different approach by Huang *et al.* employs nanoparticle surfactants with polymeric surface modifiers of different molecular weights.¹³

The new approaches of forming bijels either by STriPS or simple shaking have a key step to simplify bijel formation in common: The use of surfactants to adjust the wettability of the nanoparticles *in-situ* for the liquid scaffold stabilization.^{5,13–15} *In-situ* surface modification allows for a simple control over the nanoparticle wettability, essential for bijel stabilization, as the particles are required to adopt a near-neutral contact angle (CA $\sim 90^\circ$) to stabilize the percolating interface.^{1,24}

Though extensive work has been done on the stabilization of discrete emulsion droplets with either hydrophilic or hydrophobic particles via the *in-situ* surfactant modification of nanoparticles,^{25–31} research on the requirements to stabilize bijels with particles of different initial wettability by action of *in-situ* modifiers is limited. Research on the bijel structure dependence on the initial particle wetting properties is of great interest for many applications since, for example, catalyst particles intended for use in bijel based Pickering interfacial catalysis can have a wide range of surface wettabilities.^{23,32}

Here, we investigate the criteria for the *in-situ* surface modification of nanoparticles of different initial wettabilities to stabilize bijels formed by Solvent Transfer Induced Phase Separation (STriPS). For our study we tune the initial wettability of model silica particles from (i) moderately hydrophobic to (ii) strongly hydrophilic. Then, we investigate the type and concentration of *in-situ* modifying quaternary ammonium surfactants allowing for bijel formation with these particles.

Silica particles are functionalized with hydrophobic 3-(Trimethoxysilyl) propyl acrylate groups, and hydrophilic 3-glycidoxypropyltrimethoxysilane groups (see schematic in Fig. 1a). This wide range of initial surface properties is proposed as a model system to mimic the stabilization of bijels with potential catalyst particles^{32–37}.

Surprisingly, we find that acrylate functionalized silica nanoparticles allow for the temporary stabilization STriPS bijels without the use of *in-situ* surface modifiers. However, to obtain long term stability, *in-situ* surface modification of the nanoparticles with short chain quaternary ammonium surfactants is needed. Moreover, we show how extremely hydrophilic glycerol-coated nanoparticles require strongly hydrophobic quaternary ammonium surfactants as *in-situ* modifiers to stabilize bijels.

Last, we demonstrate how bijels with functionalized nanoparticles enhance bijel stability over wide pH ranges by cross-linking the interfacial particles. By functionalizing the particles used for making bijels, novel, robust, and versatile bijel materials can be derived for diverse applications such as drug encapsulation, controlled release of active ingredients, and Pickering interfacial catalysis.

2 Experimental methods

2.1 Materials

Silica nanoparticles (22nm Ludox TMA), hexadecyltrimethylammonium bromide (C₁₆TAB) with purity >98%, dihexadecyl dimethylammonium bromide (C₁₆)₂TAB, dodecyltrimethylammonium bromide (C₁₂TAB), diethyl phthalate (DEP, 99.5%), Nile red, 2-hydroxy-2-methylpropiophenone (HMP), 1,4-butanediol diacrylate (BDA), deionized water and pure ethanol 200 proof (>99.5%) were used for all experiments. 3-(Trimethoxysilyl) propyl acrylate (TPA, 92%) and 3-Glycidoxypropyl-trimethoxy silane (GPO, $\geq 98\%$) were purchased from Sigma-Aldrich and used as received.

2.2 Surface modification of silica nanoparticles

Silica nanoparticle dispersions, comprising water (33.3 v/v), ethanol (38.1 v/v), acetic acid (33.3 v/v) and Ludox TMA (9.5 v/v) were mixed in tightly sealed glass bottles and placed in a 70°C heating bath under constant stirring. Nitrogen was bubbled through the mixture for 10 mins. To functionalize the nanoparticles, calculated concentrations of functional monomers (3-trimethoxy propyl acrylate (TPA) or 3-glycidoxypropyltrimethoxysilane (GPO)) were introduced to the nanoparticle dispersions and stirred over-night, resulting in the silanization of hydrophobic (acrylate) or hydrophilic (glycerol) nanoparticles. After 12 hours, DI water of same volume as the reactant mixture was added to the acrylate-functionalized silica nanoparticles, resulting in particle sedimentation. The sediment was subsequently washed in DI water for three consecutive times (centrifugation, redispersion cycles). After the last washing step, the aqueous supernatant was decanted, and ethanol was added to the sediment. The samples were shaken

vigorously and ultra-sonicated to re-disperse the functionalized particles, followed by dialysis in ethanol (200 proof) for 12 hours. For glycerol-functionalized particles, the reaction mixture was partially evaporated to half of its original volume after 12-hour reaction. Then, washing was realized by three sequential dialysis steps in water at pH 3.

2.3 Preparation of Stock Solutions

Dialyzed concentrates of acrylated particles in ethanol and glycerol particles in water (both ~50wt% particles) are used as stock dispersions. To prepare surfactant solutions, calculated molar concentrations of the chosen surfactants (~100mM (C₁₆)₂TAB, ~200mM for C₁₆TAB and C₁₂TAB) are prepared in ethanol (200 proof).

2.4 Ternary Liquid mixture preparation and bijel fabrication

1.5 ml of ternary fluid mixtures at critical compositions of the oil, water, and solvent are prepared and mixed together with the functionalized silica nanoparticles (wt% = 37.5), which are used to fabricate the STRIPS bijels. The fractions of oil (ϕ_o), water (ϕ_w) and ethanol (ϕ_e) used to prepare the ternary mixtures for each of the acrylate particles were as follows: 20%-ASNs ($\phi_o = 0.32$, $\phi_w = 0.18$, and $\phi_e = 0.50$) and for 40%- and 60%-ASNs ($\phi_o = 0.27$, $\phi_w = 0.24$ and $\phi_e = 0.49$), indicated as points "A" and "B" respectively in Fig 1e. For the ternary mixtures made with the hydrophobic acrylated silica nanoparticles (20%, 40% and 60%), STRIPS bijel fibers were fabricated with or without the inclusion of surfactants. When surfactants were required, molar concentrations of the cationic alkyl surfactants (cetyltrimethylammonium bromide) were used accordingly. For hydrophilic glycerol-functionalized silica nanoparticles (GSNPs), we varied both the surfactant type (hydrocarbon chain and length) and their respective concentrations when the ternary mixtures were prepared. The bijel fiber extrusion process entailed the use of custom made microcapillary devices with polymeric coatings, as earlier reported.¹⁸ To polymerize the fabricated STRIPS bijel fibers, we added the photo initiator (HMPP) to the ternary mixture compositions and exposed them to UV light (~5 minutes), resulting in the conversion of the monomeric oil phase (BDA) into a solid polymer.

2.5 Characterization

To obtain high resolution confocal laser scanning micrographs (CLSM) of the polymerized bijel fibers, we conducted refractive index (RI) matching by soaking the UV-polymerized fibers in ethanol (200 proof) overnight and subsequently in diethyl phthalate (DEP). Highly pixelated confocal images were obtained after the confocal scans, 3D reconstructions of the bijel structures are made to obtain efficient characterization of the bicontinuous morphologies. We crop the z-stack high resolution images of the resulting CLSM data in a stepwise fashion and process them into three-dimensional figures. Sessile drop contact angle measurements are taken for each of the functionalized SNPs by using an optical tensiometer (Attention Theta, by Biolin Scientific), operated at room temperature. A thin film of either hydrophobic (ASNs) or

hydrophilic (GSNPs) particles dispersed in ethanol is spread on a glass slide and dried for approximately 30 minutes. Drops of DI water are deposited on the nanoparticle films and the resulting contact angles measured. For the glycerol functionalized nanoparticles (1 wt%), zeta potential measurements in dependence of pH are carried out to investigate their surface charges (of 20%-GSNs and 90%-GSNs) by using a Malvern Zetasizer 200 instrument at 25°C. The pH is adjusted by adding 0.1M NaOH to the aqueous particle dispersions under constant stirring. To characterize robust GSNP-bijels, CLSM was used to obtain time series of bijel structures (crosslinked and non-crosslinked) affected by increase in pH. A high-speed camera connected to an optical microscope (Nikon Diaphot 300) was used to capture micrographs of bijels undergoing fluid remixing.

Results and Discussion

Controlled initial wettabilities of nanoparticles are obtained by treatment with organofunctional alkoxy silane molecules. To this end, 22 nm sized Ludox TMA silica nanoparticles (SNPs) are silanized with either 3-(Trimethoxysilyl) propyl acrylate (TPA) or Glycidoxypropyl trimethoxy silane (GPO) to render the particles partially hydrophobic (TPA) or hydrophilic (GPO) (See schematic in Fig. 1a). Specific concentrations of TPA or GPO are introduced in a reaction vessel containing water, ethanol, acetic acid, and a dispersed fraction of the Ludox nanoparticles. The amounts of TPA or GPO added are selected based on the calculated amounts of silanol groups on the nanoparticles (see Figure SI 1 and Supplementary Note 1).³⁸ We define the percentage of coverage as the degree of TPA or GPO added to functionalize a corresponding stoichiometric percentage of silanol groups on the nanoparticles. Fig. 1b shows the results of our acid-base titrations, revealing that the added percentages of TPA translate to ~94% coverage of the available silanol groups (see Supplementary Note 2).

The stark contrast in wettability for the acrylate functionalized nanoparticles (ASNs) and glycerol functionalized nanoparticles (GSNs) is demonstrated by macroscopic contact angle measurements at a pH value of ~3. A thin particle film is deposited on a glass slide and the contact angle of a sessile water droplet on the film is measured. Fig. 1c shows that the contact angles for ASNs range from 50 – 90 degrees, indicating their partially hydrophobic character. Importantly, an increase of the degree of acrylate functionalization increases the contact angle and hydrophobic nature. In contrast, the contact angles for the GSNs range from 5 to 15 degrees, indicating their hydrophilic character (Fig. 1c).

In our study, bijels are generated via Solvent Transfer Induced Phase Separation (STRIPS).¹⁸ STRIPS requires the rapid injection of a homogeneous ternary mixture into a continuous stream of water to make bijels. The hydrophobic (oil) and hydrophilic (water) components are mixed via a solvent (ethanol), which includes a dispersed suspension of functionalized nanoparticles to make a homogeneous ternary

mixture. When the ternary mixture is extruded into a continuous stream of water, the solvent (ethanol) is extracted into the surrounding water, leading to phase separation. As demixing proceeds, the nanoparticles are swept onto the liquid-liquid interface, where they accumulate and jam to arrest the bicontinuous oil/water network (see schematic in Fig. 1d). Continuously fabricated STRIPS bijel fibers can be polymerized and used for multiple applications.^{5,13}

In the following, we present the results of our investigation of stabilizing STRIPS bijels, first with acrylate-functionalized particles, and second with glycerol functionalized particles. It is important to stress that our results are valid for particles with surfaces conditioned at acidic pH value ($\text{pH} < 3$). Here, the majority of the remaining silanol groups of the partially functionalized silica nanoparticles are protonated.

3.1 Stabilization of bijels with partially hydrophobic (acrylate functionalized) nanoparticles.

Acrylated nanoparticles are found to affect the ternary liquid phase equilibrium by decreasing the miscibility. A suspension of ASNPs in ethanol is mixed with 1,4 butanediol diacrylate (BDA), pure ethanol, and water. A miscible particle-ternary mixture suspension remains clear, indicating homogeneous particle dispersion and effective mixing of the liquid and solid components. The miscibility of the mixture is dictated by the binodal line (indicated as (2)) in the ternary liquid phase diagram displayed in Fig. 1e. In contrast to the liquid mixture composed of only the liquids BDA, ethanol, and water (indicated as (1)), the binodal line is shifted upwards with added acrylated particles. This is likely due to the overall increase in the hydrophobic constituents (oil (BDA) + acrylate particles) included in the ternary mixture, which required a corresponding increase in the fraction of ethanol needed for homogeneous mixing.

Solvent Transfer Induced Phase Separation (STRIPS) is carried out with ternary compositions indicated in the ternary phase diagram, as indicated by the points, "A" for 20%-ASNP and "B" for both 40% and 60%-ASNPs (see Fig. 1e), plus 0.4 wt-% of the radical photo initiator 2-hydroxy-2-methylpropionophenone (HMPP) and < 0.1 wt-% Nile Red. The ternary mixtures are extruded as fibers via a coaxial glass capillary device and collected in a water-filled vial.¹⁴ Within less than two minutes after extrusion, the fibers are irradiated with high intensity UV-light (5 mins, 340 nm, > 20 W/cm²) for polymerization of the BDA. The polymerized fibers are washed with ethanol and immersed in diethyl phthalate to obtain optical transparency for further characterization.

Confocal laser scanning microscopy (CLSM) reveals well-defined bicontinuous channel morphologies for all degrees of acrylation investigated here (20%-ASNP, 40%-ASNP and 60%-ASNP) (Fig. 2). This finding shows how the inherent hydrophobicity of the ASNPs enables the stabilization of bicontinuous liquid structures by the particles alone. Our result contrasts with previous findings, where the addition of cationic surfactants in combination with unmodified silica particles was needed to obtain bijel morphologies.^{5,14,23}

The fibers have asymmetric pore size distributions, with small pores at the surface and larger pores towards the inside. This trend is quantified in Fig. 2b, showing measurements of the oil domain sizes from the surface (at 0 μm) to the equatorial regions (at $\sim 40 \mu\text{m}$). Similar asymmetric structures of STRIPS bijels have been found in earlier reports with surfactant-modified particles,^{5,14} further extending their potential applications in separations, especially where size-selective transport is required.³⁹

The internal oil domains become larger in size, show more interconnectivity, and more strongly resemble the spinodal patterns of the phase separation with increasing degree of particle acrylation. (Fig. 2a). The presence of more spinodal patterns, for example in 60%-ASNP, is likely what contributes to the overall increase in STRIPS bijel surface area when the acrylate density is increased, which is quantified in Fig. 2c (see supplementary Note 3). Also, a possible explanation for the increased volume of the oil domains is that with more hydrophobic particles, enhanced particle partitioning into the oil-rich phase takes place. Correspondingly, the oil-to-water volume ratio increases with respect to an increase in the acrylate density, as quantified in Fig. 2d.

When left unpolymerized, bijels formed with acrylated particles alone coarsen over time (Fig. 3). This coarsening process is significantly slower (mins to tens of mins) than the spinodal phase separation (milliseconds to seconds), indicating a gradual rearrangement of the interfacial nanoparticles. Interestingly, the coarsening dynamics are slower with particles of increasing acrylation degree. 60%-ASNP STRIPS-bijels are most stable (for up to 15 minutes), followed by 40%-ASNP (6 minutes) and lastly, 20%-ASNP (only up to 2 minutes). Long-term stability of bijels formed with acrylated particles can be achieved via addition of cationic surfactants. The coarsening observed in Fig. 3 does not take place when 1 mM hexadecyltrimethylammonium bromide (C_{16}TAB) is added to the continuous external water phase. It is likely that the remaining silanol (SiOH) groups on the surface of the nanoparticles serve as physisorption sites for the C_{16}TAB molecules, rendering them sufficiently interfacially active to permanently stabilize the bijel structure. On the other hand, irrespective of the degree of acrylation, the direct addition of C_{16}TAB to the ternary mixture does not allow for bijel formation, and instead results in viscoelastic oil structures with interspersed water droplets, rather than bicontinuous channels (see Supplementary Note 4). This indicates excessive hydrophobicity imparted to the particles by C_{16}TAB adsorption from the ternary mixture, resulting in the formation of water-in-oil emulsions.

By replacing C_{16}TAB with dodecyltrimethylammonium bromide (C_{12}TAB), long term stability of STRIPS bijels with controllable bicontinuous morphology can be achieved. We study the effect of C_{12}TAB addition to the initial ternary mixture in the following. Fig. 4 shows confocal 3D reconstructions of STRIPS bijels fabricated with particles of variable degrees of acrylation in dependence of the C_{12}TAB concentrations in the initial ternary casting mixture. As opposed to C_{16}TAB , a wider range of surfactant concentrations facilitates the formation of

nodular bicontinuous within the fibers. For example, for 20%-ASNPs, up to ~40 mM C_{12} TAB results in the formation of bicontinuous structures.

The initial hydrophobicity of the nanoparticles determines the maximum allowable additional hydrophobicity imparted by the surfactant for bijel stabilization. For each degree of particle acrylation, a characteristic threshold exists, above which no bicontinuous nodular oil/water channels can be formed. The higher the degree of acrylation, the lower this threshold surfactant concentration. Bijels are not formed for 60%-ASNPs above 20 mM C_{12} TAB, for 40% ASNPs above 30 mM C_{12} TAB or for 20% ASNPs above 45 mM C_{12} TAB. It is likely that above these threshold surfactant concentrations, excessive adsorption of C_{12} TAB renders the nanoparticles too hydrophobic to stabilize bicontinuous structures. This finding indicates that the initial hydrophobicity of the nanoparticles puts a limit to the additional hydrophobicity imparted by the surfactant.

The surface pore sizes of the ASNP bijel fibers decrease with an increase in the surfactant (C_{12} TAB) concentration in the range below the concentration threshold, whereas their surface oil domain sizes increase with an increase in the degree of acrylation and pH (see Supplementary Note 5).

An interesting observation is that with added C_{12} TAB, the bijel fibers often have hollow interiors (Fig. 4). We believe, this can be related to the accumulation of water rich phase in the centre of the fiber during STRIPS. Electron microscopy shows that the surface pores of the bijels formed with C_{12} TAB are clogged by aggregated excess silica particles. This pore clogging can result in a significant barrier for the diffusion of solvent to the external water phase. As a result, the solvent is trapped in the middle of the fiber and generates a hollow interior.

This pore clogging effect can be suppressed in part by the addition of propanol to the continuous water phase. SEM images show that with the addition of 10 vol-% propanol, open surface pore structures are formed (see Fig. S17 in Supplementary Note 6). This finding is analogous to the pore opening effect with ethanol addition to the continuous phase found in previous reports.⁵ However, in the present work, ethanol addition did not open the surface pores as significantly as propanol. A possible explanation is that propanol reduces the aggregation of the acrylate functionalized particles by suppressing the interaction of the adsorbed C_{12} TAB chains.

3.2 Stabilization of bijels with hydrophilic (glycerol functionalized) nanoparticles.

Besides hydrophobic particles as stabilizers, potential catalyst particles for the stabilization of bijels can also be of hydrophilic nature. To investigate the requirements to stabilize STRIPS bijels with hydrophilic particles, we employ glycerol functionalized silica particles as model systems. Silica nanoparticles (22 nm diameter) are functionalized with 3-Glycidoxypropyltrimethoxy-silane (GPO). The degree of particle functionalization by glycerol groups is controlled to tune the particle wettabilities within the hydrophilic regime. Zeta potential measurements show that the density of the glycerol

groups affects the electrophoretic mobility of the functional nanoparticles (Supplementary Note 7).

Glycerol-functionalized nanoparticles are not capable of stabilizing bijels on their own, irrespective of the degree of functionalization. Therefore, we test the effect of adding cationic alkylammonium bromide surfactants on the bijel stabilization capability of the particles. The surfactant (C_{16} TAB) does not impart enough hydrophobicity to glycerol functionalized nanoparticles for bijel stabilization. We show this by injecting 50 microliters of the ternary mixture with a pipette into water. Fig. 5 shows confocal micrographs of the resulting structures formed with particles of 50% glycerol functionalization.

Increasing the C_{16} TAB concentration up to 30 mM in the ternary mixture does not lead to the stabilization of bicontinuous structures. This is likely a consequence of the large amount of hydrophilic hydroxyl (OH) groups on the surface of the nanoparticles. However, we find that viscoelastic nonspherical droplet structures are formed at ~30 mM C_{16} TAB, indicating interfacial particle attachment and jamming.

Interestingly, bijels can be stabilized with glycerol functionalized nanoparticles in combination with cationic double chain surfactants. Fig. 5 shows that upon addition of 21 mM didodecyldimethylammonium bromide ($(C_{12})_2$ TAB) to the ternary mixture with glycerol functionalized nanoparticles, bijel-like structures can be obtained.

Furthermore, when the hydrocarbon chain lengths of the dual-chained surfactants are increased (dihexadecyldimethylammonium bromide ($(C_{16})_2$ TAB), further reduction of the surfactant concentration (~13 mM) results in the formation of bijel-like structures. Moreover, we observed that for the same type of surfactant ($(C_{16})_2$ TAB), higher concentrations were required for higher degrees of glycerol functionalization on the silica nanoparticles (Supplementary Note 8). This is likely due to the surfactant adsorption limitations encountered for higher glycerol degrees, as well as the extreme hydrophilicity imparted by the abundance of hydroxyl (OH) groups. As opposed to ASNP bijels with small surface pores (< 2 μ m), bijels made with hydrophilic glycerol particles have significantly open surface pore structures (~12 μ m), as a result of the easy dispersibility of GSNPs in the external continuous water phase (Fig. 6).

4 Robust bijels via interfacial nanoparticle crosslinking.

The confocal micrograph time series in Figure 7a shows that glycerol particle stabilized bijels coarsen upon adding sodium hydroxide to the continuous water phase (pH increase from 3 to 10). The strongly negatively charged silica surface at pH 10 likely increases the adsorbed amount of $(C_{16})_2$ TAB on the particles, changing their contact angle.^{29,40} Particles with contact angles deviating from 90 degrees cannot stabilize bicontinuous oil/water channels, as they introduce a preferential curvature to the interface.^{2,41} Stability of bijels against changes in solution pH is achieved by particle cross-linking. We demonstrate this on the example of bijels stabilized with glycerol functionalized nanoparticles.

Particle cross-linking is achieved by Toluene 2,4-diisocyanate terminated poly(propylene glycol) (TDPPO, Mn 2,300 g/mol) (see schematic in Fig. 7b).⁴² TDPPO is added to the initial ternary mixture and the STRIPS process is carried out. TDPPO likely partitions into the BDA rich phase during STRIPS due to its hydrophobic polypropylene spacer. The bijel is stored at room temperature for 12 hours for the reaction of the isocyanate groups with the hydroxyl groups to take place. TDPPO crosslinked bijels are stable under high pH conditions, which is shown by the preservation of the bicontinuous morphology in the time series in Figure 7c. Furthermore, the robustness of the crosslinked bijels are observed by their stability after remixing the oil and water via addition of ethanol to the continuous water phase. After TDPPO cross-linking, ethanol addition dissolves the oil, but the reinforced percolating nanoparticle framework remains intact, as observed via light microscopy (Fig. 7d). By increasing the pH of the crosslinked particles following fluid remixing, and subsequently introducing a positively charged dye (Rhodamine 110), the preserved bicontinuous scaffold is observed under confocal laser scanning microscopy, which shows that not only is the bijel surface preserved, but the internal regions are as well (see Supplementary Note 9). In contrast, the non-crosslinked glycerol particle stabilized bijels collapsed entirely upon the addition of ethanol (Fig. 7e).

5 Conclusion

In summary, STRIPS bijel formation was studied with silica nanoparticles of different surface functionalizations to investigate the effect of initial particle wettability on STRIPS bijel stabilization criteria. 3-(Trimethoxysilyl) propyl acrylate-functionalized silica particles were investigated to study bijel stabilization with particles of partially hydrophobic wettability. We find that acrylate-functionalized particles facilitate temporary stabilization of STRIPS bijels on their own. Long-term stability can be imparted by the addition of the mildly hydrophobic cationic surfactant dodecyldimethylammonium bromide. In contrast, our results on STRIPS bijel formation with strongly hydrophilic particles containing 3-glycidoxypropyltrimethoxysilane groups show the opposite requirement for the surfactant. Here, only highly hydrophobic double chain surfactants (dihexadecyldimethylammonium bromide) facilitate the stabilization of STRIPS bijels. Last, we demonstrate how glycerol-functionalized silica particles facilitate interfacial particle cross-linking by isocyanate chemistry. After cross-linking, structural integrity of the STRIPS bijel nanoparticle scaffold is preserved when pH is increased. This holds true even after remixing of the constituent immiscible fluids of the bijel.

Our study shows how different types of surfactants facilitate the stabilization of bicontinuous emulsions with particles of various initial wettabilities. Our findings will progress future research in designing STRIPS bijel structures by selecting appropriate surfactants for the formation of robust next-generation STRIPS bijels. We are currently investigating methods to obtain fluid transport in robust STRIPS bijels for biphasic applications.

Conflicts of Interest

There are no conflicts to declare.

Acknowledgment

Acknowledgement is made to the National Science Foundation for support of this research under award number 1751479. This work was supported by NSF-CAREER award number 1751479.

References

- 1 K. Stratford, R. Adhikari, I. Pagonabarraga, J. C. Desplat and M. E. Cates, *Science*, 2005, **309**, 2198–2201.
- 2 E. M. Herzig, K. A. White, A. B. Schofield, W. C. K. Poon and P. S. Clegg, *Nature Materials*, 2007, **6**, 966–971.
- 3 P. S. Clegg, E. M. Herzig, A. B. Schofield, S. U. Egelhaaf, T. S. Horozov, B. P. Binks, M. E. Cates and W. C. K. Poon, *Langmuir*, 2007, **23**, 5984–5994.
- 4 C. A. L. Colard, R. A. Cave, N. Grossiord, J. A. Covington and S. A. F. Bon, *Advanced Materials*, 2009, **28**, 2894–2898.
- 5 M. F. Haase, H. Jeon, N. Hough, J. H. Kim, K. J. Stebe and D. Lee, *Nature Communications*, 2017, **8**, 1234.
- 6 T. J. Thorson, E. L. Botvinick and A. Mohraz, *ACS Biomaterials Science & Engineering*, 2018, **4**, 587–594.
- 7 S. Zekoll, C. Marriner-Edwards, A. K. O. Hekselman, J. Kasemchainan, C. Kuss, D. E. J. Armstrong, D. Cai, R. J. Wallace, F. H. Richter, J. H. J. Thijssen and P. G. Bruce, *Energy & Environmental Science*, 2018, **11**, 185–201.
- 8 J. R. Wilson, J. S. Cronin, A. T. Duong, S. Rukes, H. Y. Chen, K. Thornton, D. R. Mumm and S. Barnett, *Journal of Power Sources*, 2010, **195**, 1829–1840.
- 9 M. N. Lee and A. Mohraz, *Advanced Materials*, 2010, **22**, 4836–4841.
- 10 J. A. Witt, D. R. Mumm and A. Mohraz, *Journal of Materials Chemistry A*, 2016, **4**, 1000–1007.
- 11 D. Cai, F. H. Richter, J. H. J. Thijssen, P. G. Bruce, & P. S. Clegg, P. S. (2018). Direct transformation of bijels into bicontinuous composite electrolytes using a pre-mix containing lithium salt. *Materials Horizons*, 5(3), 499–505.
- 12 J. W. Tavacoli, J. H. J. Thijssen, A. B. Schofield and P. S. Clegg, *Advanced Functional Materials*, 2011, **21**, 2020–2027.
- 13 C. Huang, J. Forth, W. Wang, K. Hong, G. S. Smith, B. A. Helms and T. P. Russell, *Nature Nanotechnology*, 2017, **12**, 1060–1063.
- 14 M. F. Haase, K. J. Stebe and D. Lee, *Advanced Materials*, 2015, **27**, 7065–7071.
- 15 D. Cai, P. S. Clegg, T. Li, K. A. Rumble and J. W. Tavacoli, *Soft Matter*, 2017, **13**, 4824–4829.
- 16 S. Gam, A. Corlu, H. J. Chung, K. Ohno, M. J. A. Hore and R. J. Composto, *Soft Matter*, 2011, **7**, 7262–7268.
- 17 H. J. Chung, J. Kim, K. Ohno and R. J. Composto, *ACS Macro Letters*, 2012, **1**, 252–256.
- 18 C. C. Barker, *PEDIATRICS*, 2005, **115**, 1341–1346.
- 19 N. Hijnen, D. Cai and P. S. Clegg, *Soft Matter*, 2015, **11**,

- 4351–4355.
- 20 L. Imperiali, C. Clasen, J. Fransaer, C. W. Macosko and J. Vermant, *Materials Horizons*, 2014, **1**, 139–145.
- 21 H. Firoozmand and D. Rousseau, *Food Hydrocolloids*, 2015, **48**, 208–212.
- 22 L. Li, C. Miesch, P. K. Sudeep, A. C. Balazs, T. Emrick, T. P. Russell and R. C. Hayward, *Nano Letters*, 2011, **11**, 1997–2003.
- 23 G. Di Vitantonio, T. Wang, M. F. Haase, K. J. Stebe and D. Lee, *ACS Nano*, 2018, **13**, 26–31.
- 24 P. S. Clegg, *Journal of Physics Condensed Matter*, 2008, **20**, 113101.
- 25 V. O. Ikem, A. Menner and A. Bismarck, *Angewandte Chemie - International Edition*, 2008, **47**, 8277–8279.
- 26 Z. G. Cui, L. L. Yang, Y. Z. Cui and B. P. Binks, *Langmuir*, 2010, **26**, 4717–4724.
- 27 M. Xiao, A. Xu, T. Zhang and L. Hong, *Frontiers in Chemistry*, 2018, **6**, 225.
- 28 M. F. Haase, D. Grigoriev, H. Moehwald, B. Tiersch and D. G. Shchukin, *Journal of Physical Chemistry C*, 2010, **114**, 17304–17310.
- 29 A. Maestro, E. Guzmán, E. Santini, F. Ravera, L. Liggieri, F. Ortega and R. G. Rubio, *Soft Matter*, 2012, **8**, 837–843.
- 30 B. P. Binks and J. A. Rodrigues, *Angewandte Chemie - International Edition*, 2007, **46**, 5389–5392.
- 31 Y. Zhu, J. Jiang, K. Liu, Z. Cui and B. P. Binks, *Langmuir*, 2015, **31**, 3301–3307.
- 32 M. Pera-Titus, L. Leclercq, J.-M. Clacens, F. De Campo and V. Nardello-Rataj, *Angewandte Chemie International Edition*, 2015, **54**, 2006–2021.
- 33 W.-J. Zhou, L. Fang, Z. Fan, B. Albela, L. Bonneviot, F. De Campo, M. Pera-Titus and J.-M. Clacens, *Journal of the American Chemical Society*, 2014, **136**, 4869–4872.
- 34 L. Leclercq, A. Mouret, A. Proust, V. Schmitt, P. Bauduin, J. M. Aubry and V. Nardello-Rataj, *Chemistry - A European Journal*, 2012, **18**, 14352–14358.
- 35 Y. Yang, W. J. Zhou, A. Liebens, J. M. Clacens, M. Pera-Titus and P. Wu, *Journal of Physical Chemistry C*, 2015, **119**, 25377–25384.
- 36 S. Drexler, J. Faria, M. P. Ruiz, J. H. Harwell and D. E. Resasco, *Energy and Fuels*, 2012, **26**, 2231–2241.
- 37 T. Riittonen, E. Toukoniitty, D. K. Madnani, A.-R. Leino, K. Kordas, M. Szabo, A. Sapi, K. Arve, J. Wärnå and J.-P. Mikkola, *Catalysts*, 2012, **2**, 69–84.
- 38 E. F. Vansant, P. Van Der Voort and K. C. Vrancken, *Characterization and chemical modification of the silica surface*, Elsevier, 1995, vol. 93.
- 39 K. V. Peinemann, V. Abetz and P. F. W. Simon, *Nature Materials*, 2007, **6**, 992.
- 40 V. Poulichet and V. Garbin, *Proceedings of the National Academy of Sciences*, 2015, **112**, 5932–5937.
- 41 M. Destribats, S. Gineste, E. Laurichesse, H. Tanner, F. Leal-Calderon, V. Héroguez and V. Schmitt, *Langmuir*, 2014, **30**, 9313–9326.
- 42 K. L. Thompson, S. P. Armes, J. R. Howse, S. Ebbens, I. Ahmad, J. H. Zaidi, D. W. York and J. A. Burdis, *Macromolecules*, 2010, **43**, 10466–10474.

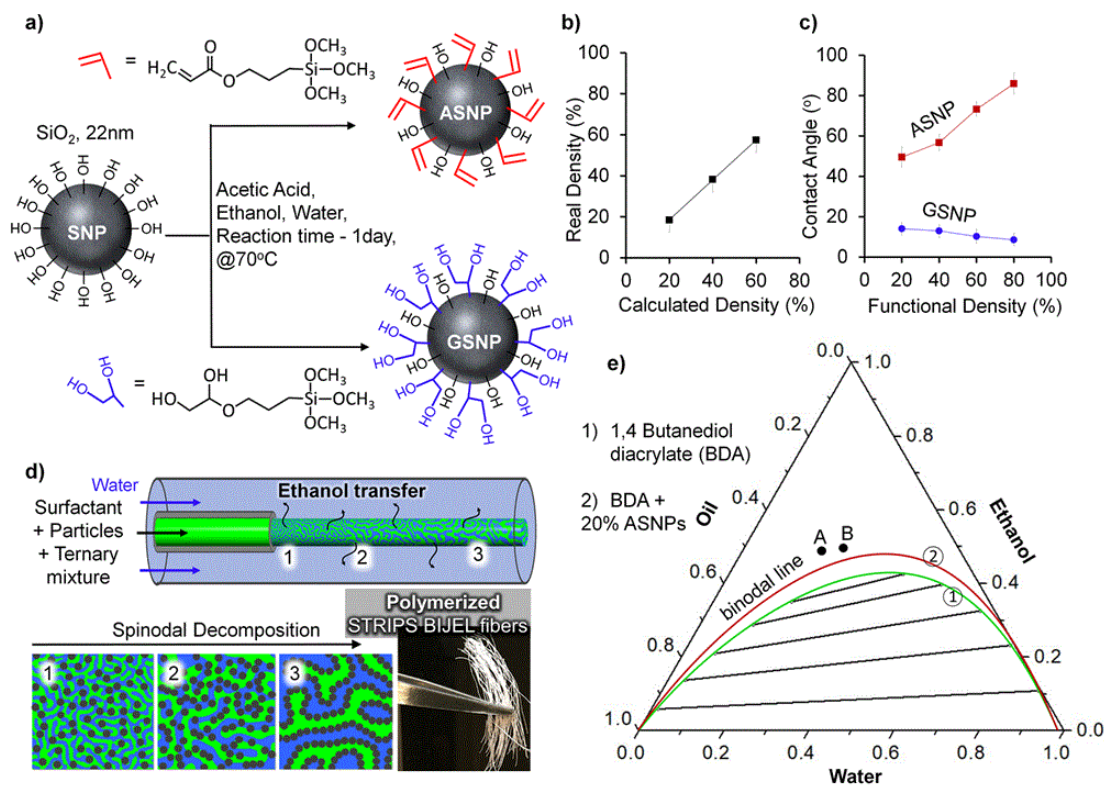


Fig. 1: Nanoparticle modification and STRIPS bijel fabrication. (a) Surface modification of 22nm Ludox TMA silica nanoparticles (SNP) with acrylate or glycerol groups, rendering the particles partially hydrophobic (ASNP) or hydrophilic (GSNP) respectively. (b) Results from acid-base titration experiments to derive the percentage of silanol groups on functionalized SNPs. (c) Results from sessile drop contact angle measurements for both acrylate and glycerol functionalized particles of varying degree of functionalization (conducted on a thin film deposition of functionalized particle dispersion on a glass slide). (d) Fabrication method of STRIPS bijels by co-axial extrusion of ternary mixtures into a stream of water within a coaxial microcapillary device. (e) Measured ternary phase diagram with binodal and tie lines of the liquid system, oil (1,4 butanediol diacrylate (BDA)), water and solvent (ethanol). The initial ternary compositions used for STRIPS in this work is indicated by the black points on the binodal line ("A" for 20% - ASNP and "B" for both 40% and 60% - ASNPs). The binodal line position of BDA (indicated as (1)), is moved upwards due to the addition of hydrophobic acrylate functionalized silica nanoparticles (indicated as (2)).

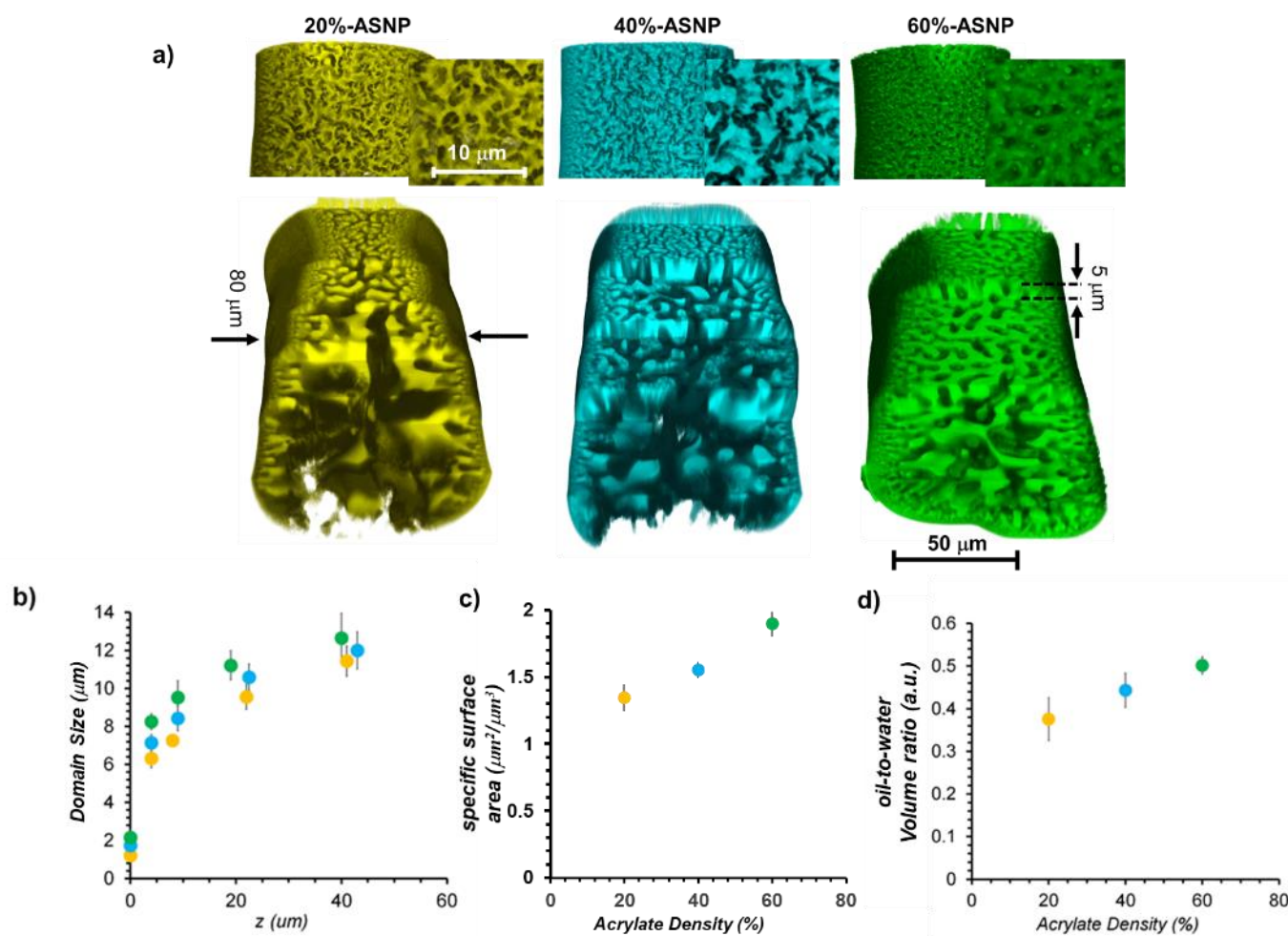


Fig. 2: STriPS bijels stabilized solely with acrylate functionalized silica nanoparticles (ASNPs). (a) 3D confocal laser scanning microscopy reconstructions of surfactant-free STriPS bijel fibers. The 3D reconstructions of the cylindrical fibers were cut at different height levels to reveal the internal morphologies (see supplementary methods). Samples were fabricated by using particles with varying acrylate densities (20%-ASNP, 40%-ASNP and 60%-ASNP). (b) Oil domain size measurements with respect to confocal z positions of the respective ASNP-STriPS bijel fibers in (a), where the data points are indicated by the respective colour codes of the fiber segments. (c) The surface area measurements are estimated using 2D image analysis of equatorial slices of the respective fiber segments (also, see Supplementary Note 3). (d) The oil-to-water volume ratio of the fibers are estimated from 2D image analysis of the equatorial slices from each of the fiber segments in (a) (also see Supplementary Note 3). The error bars correspond to standard deviations of five measurements.

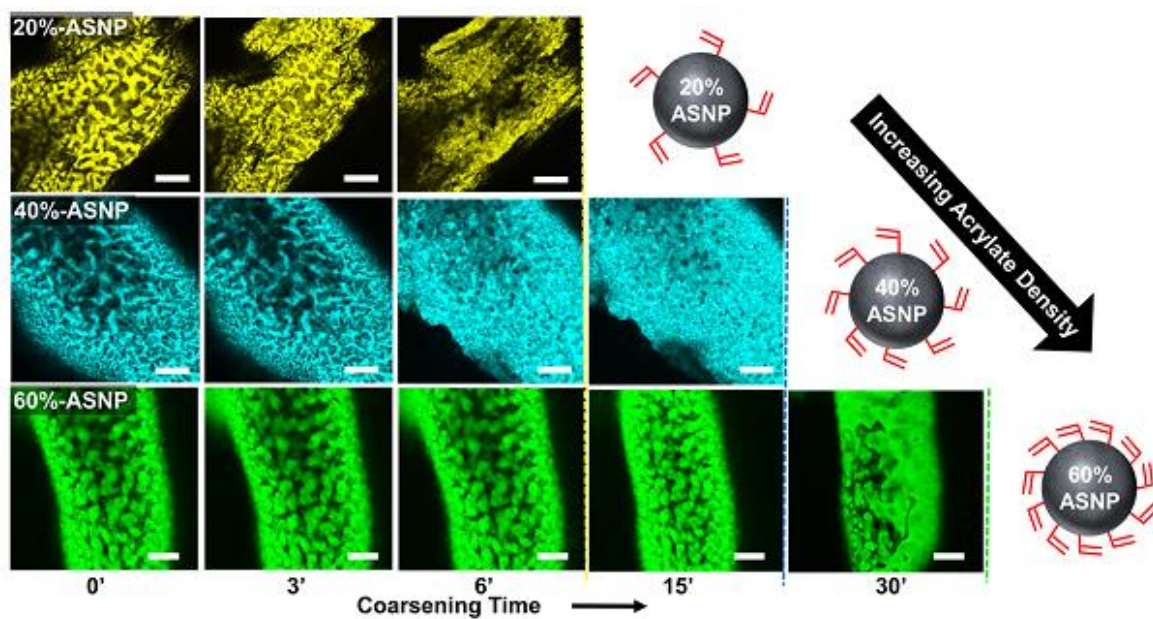


Fig. 3: Coarsening dynamics of STRIPS-bijels stabilized with acrylate silica nanoparticles. Confocal Laser Scanning Microscopy time series of coarsening bijels stabilized solely with acrylate functionalized silica nanoparticles. Onset of bijel destabilization decreases with decreasing degree of acrylate functionalization (15 mins for $\rho_{60\%}$, > 6 mins for $\rho_{40\%}$ and > 3 mins for $\rho_{20\%}$). Scale bar corresponds to 20 μm .

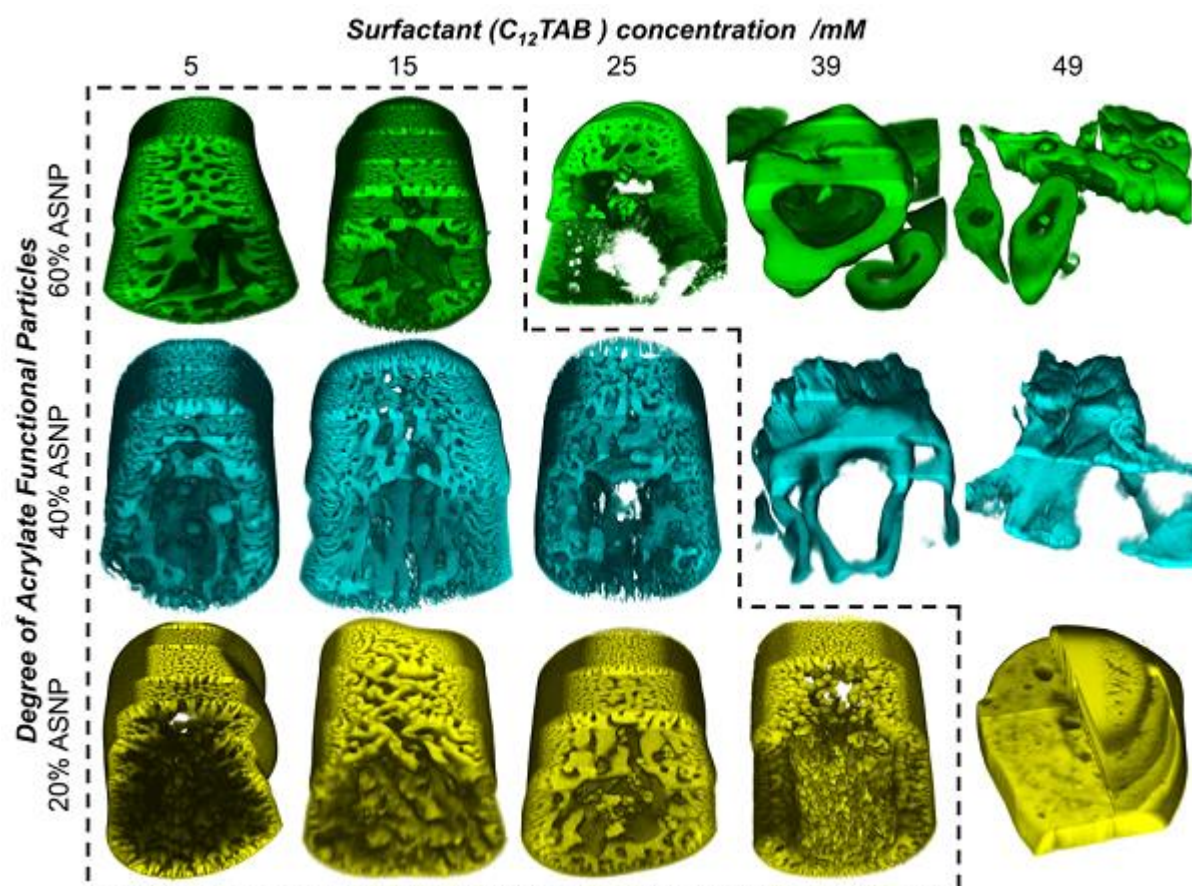


Fig. 4: Asymmetric structures of STriPS bijel fibers formed with acrylated silica nanoparticles and $C_{12}TAB$. False coloured 3D-reconstructions of STriPS bijel fiber segments stabilized with nanoparticles of different degrees of acrylation in dependence of the surfactant concentration (dodecyltrimethylammonium bromide ($C_{12}TAB$)). Particles with higher acrylate densities require relatively less surfactant concentrations (as is the case for 60% ASNP, in Fig. 4) to form bijels, whereas particles with lower acrylate densities (e.g. 20%-ASNP) can still stabilize bijels when higher surfactant concentrations are added.

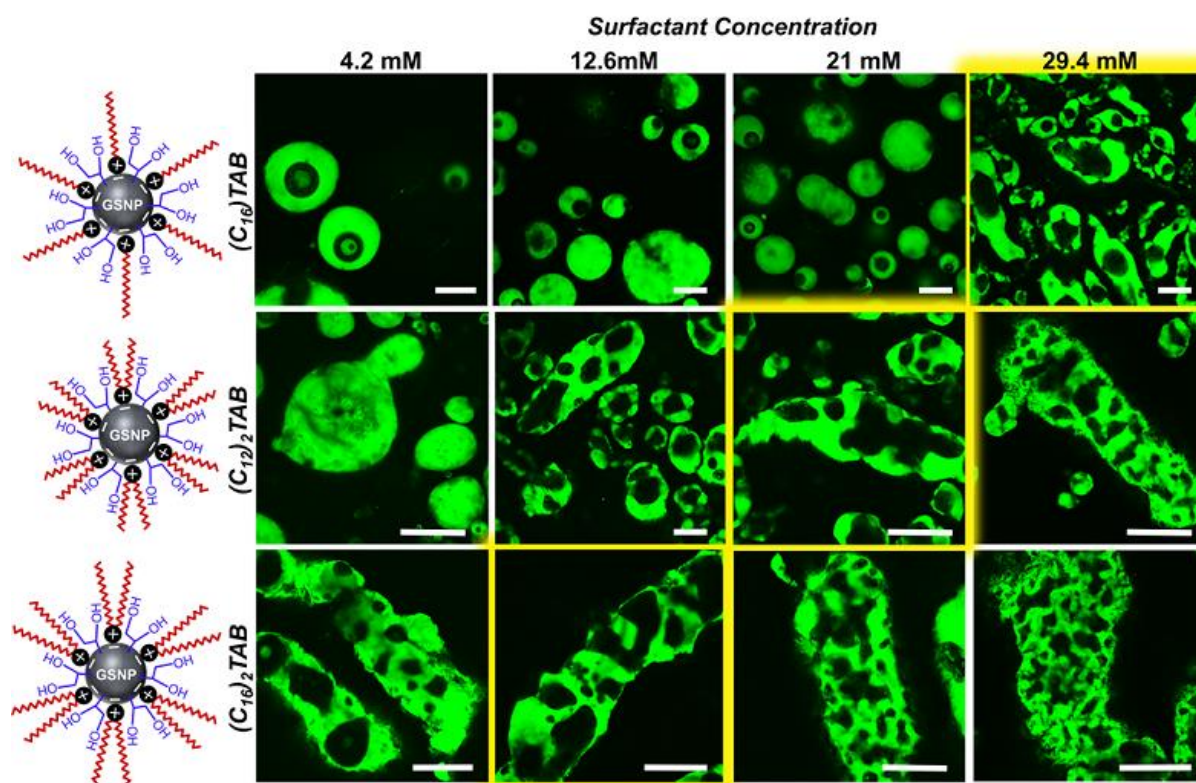


Fig. 5: STRIPS bijels stabilized with hydrophilic glycerol- functionalized silica nanoparticles. Confocal laser scanning microscopy slices of Nile Red dyed emulsion structures formed by glycerol- functionalized silica nanoparticles (50%-GSNPs) and surfactant- functionalized nanoparticles. First row: The single chain surfactants C₁₆TAB does not lead to bijel formation, irrespective of the concentration. Second row: Bijel- like structures can be obtained with the double chain surfactants didodecyldimethylammonium bromide ((C₁₂)₂TAB) above concentrations of 21 mM. Third row: The double chain surfactant dihexadecyldimethylammonium bromide ((C₁₆)₂TAB) facilitated bijel stabilization at concentrations above 12.6 mM with glycerol- functionalized nanoparticles. Scale bars correspond to 50 μ m.

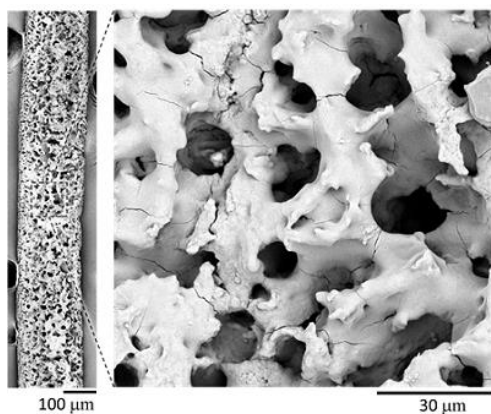


Fig. 6: Scanning Electron Micrograph (SEM) of STRIPS bijel fabricated with glycerol silica nanoparticles (50%-GSNP), showing surface pore openness. 40mM of the surfactant (C_{16})₂TAB was used in the ternary mixture composition. The continuous phase contained only 5% v/v of ethanol. On the left, is a piece of the fabricated GSNP-bijel fiber with a corresponding magnified image on the right.

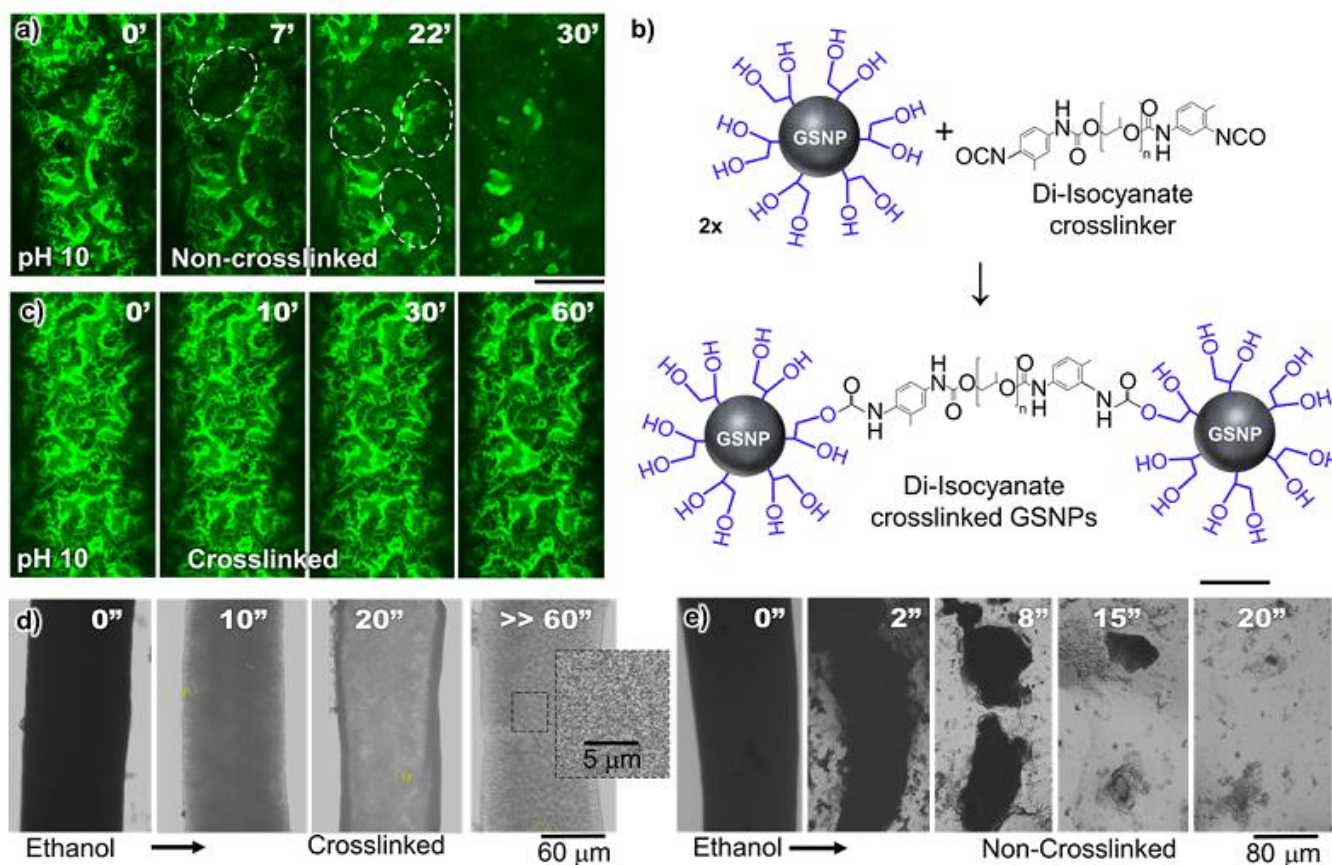


Fig. 7: Robust bijels via interfacial nanoparticle crosslinking. (a) Confocal microscopy time series showing coarsening of a glycerol-functionalized particle-stabilized bijel ($(C_{16})_2TAB$ modified) upon pH increase. (b) Schematics of isocyanate crosslinking of glycerol-functionalized silica nanoparticles. The isocyanate monomer is dissolved in the oil phase during the ternary mixture preparation prior to bijel fabrication. (c) Confocal microscopy time series showing stability of tolylene 2,4-diisocyanate terminated poly(propylene glycol) (TDPPPO) cross-linked bijel upon pH increase. (d) Light microscopy time series showing stability of the nanoparticle scaffold of TDPPPO cross-linked bijel upon oil dissolution by ethanol addition. (e) Light microscopy time series of dissolution of glycerol functionalized particle stabilized bijel upon ethanol addition.

Supporting Information

Designing Bijels formed by Solvent Transfer Induced Phase Separation with Functional Nanoparticles

Stephen Boakye-Ansah¹, Matthew Schwenger¹, Martin F. Haase¹,

¹Rowan University, Henry M. Rowan College of Engineering, Glassboro, NJ 08028 USA.

Supplementary Note 1: Calculation of the amounts of organofunctional silane added to tune the wettability of silica nanoparticles

Supplementary Note 2: Acid-Base titrations and calculations on the functionalized particles

Supplementary Note 3: Characterization of STrIPS bijel fibers.

Supplementary Note 4: Nucleated STrIPS fibers formed by addition of C₁₆TAB to the ternary mixtures

Supplementary Note 5: Surface pore and Domain size characterization of ASNP-StrIPS bijels

Supplementary Note 6: Control of excess nanoparticles at the surface of ASNP-StrIPS bijels

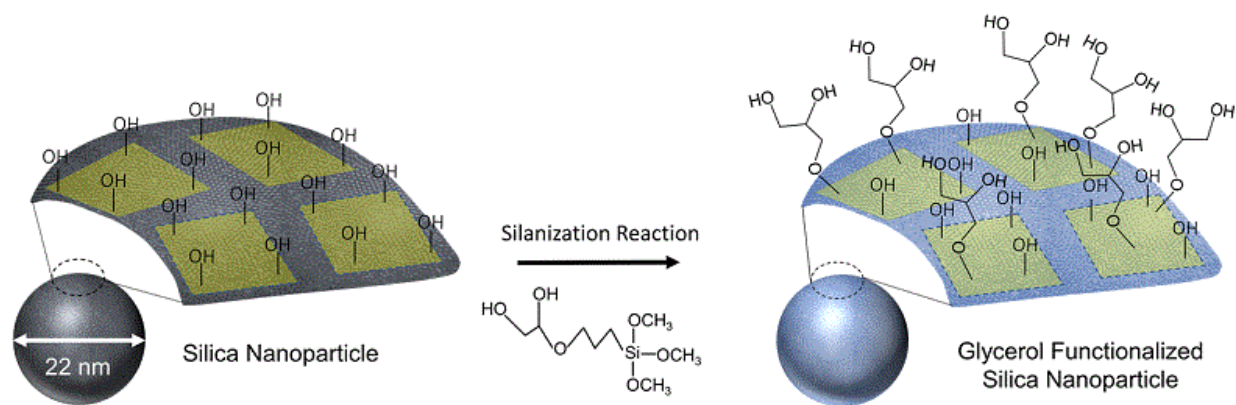
Supplementary Note 7: Surface Charge Measurements of glycerol functionalized silica nanoparticles particles.

Supplementary Note 8: Effect of glycerol density and surfactant concentration on STrIPS bijel formation.

Supplementary Note 9: Dye adsorption on crosslinked bijel scaffolds after fluid remixing

Supplementary Note 1: Calculation of the amounts of organofunctional silane added to tune the wettability of silica nanoparticles

The schematic in Supplementary Figure 1 depicts the approximated number of silanol groups per nm^2 , based on which calculations are made to functionalize the silica nanoparticles (SNPs) (22 nm) with the various organofunctional silanes.¹ As a demonstration we choose the silanization of 22 nm SNPs with Glycidoxypropyl trimethoxy silane (GPO), which we believe are distributed on the surface of the particles in relation to the degree of functionalization, hence, tuning their surface wettabilities.



Supplementary Figure 1: Depiction of silica nanoparticle spherical surface covered with silanol (Si-OH) groups. Assumption is made for 4 Si-OH groups per nm^2 and also, for an overall surface area of $150 \text{ m}^2/\text{g}$. Based on this estimation, the amount of organofunctional silane molecules is added during the silanization process, resulting in a percentage coverage (degree) of the selected functional groups. In this schematic, a 22 nm silica nanoparticle is silanized with 3-glycidoxypropyl trimethoxy silane (GPO).

The following calculations provide estimations made during the silanization of the silica nanoparticles. The total number of silanol groups (N_{SiOH}) on the silica particles is calculated as:

$$N_{\text{SiOH}} = 4 \text{ Si-OH molecules/nm}^2 \times 150 \text{ m}^2/\text{g} = \underline{\mathbf{6.0 \times 10^{20} \text{ SiOH molecules/g}}}$$

Calculation is made for the total number of SiOH molecules (n_i) (in moles per gram) by dividing

N_{SiOH} by the Avogadro's number, N_{AV} :

$$\begin{aligned} n_i &= N_{\text{SiOH}} / N_{\text{AV}} = 6.0 \times 10^{20} [\text{SiOH molecules/g}] / 6.0223 \times 10^{23} [\text{molecules/mol}] \\ &= \underline{\mathbf{9.963 \times 10^{-4} \text{ mol/g}}} \end{aligned}$$

Hence, mass of organofunctional molecules (m_{silane}) required for silanization is calculated as:

$$(m_{\text{silane}}) = n_i [\text{molecules/mol}] \times \text{molar mass } (M_i [\text{g/mol}])$$

$$m_{\text{silane}} = 9.963 \times 10^{-4} [\text{mol/g}] \times M_i [\text{g/mol}];$$

Where M_i is the molar mass of the chosen organofunctional silane.

The added mass (Δm) of silica nanoparticles (SNPs) to the reaction vessel is calculated as:

$$\Delta m_{\text{SNPs}} = \Delta V_{\text{SNPs}} \times \rho_{\text{SNPs}} \times W_{\text{SNPs}}$$

Where ΔV_{SNPs} is the volume (ml) of aqueous of SNPs dispersion (*Ludox TMA*) added; W_{SNPs} is the weight fraction of SNPs in the aqueous dispersion ($50 \text{ wt}\%$); and ρ_{SNPs} is the density of aqueous SNPs dispersion (1.23 g/ml , *Ludox TMA*).

Hence, the amount of organofunctional groups (n_{silane}) (in mols) required to tailor the wettability of the SNPs can be calculated as

$$n_{\text{silane}} = m_{\text{silane}} \times \Delta m_{\text{SNPs}} / M_i \times S$$

where S = fraction of organofunctional silane on the surface of nanoparticles, represented in this calculation as 0.2 , 0.4 and 0.6 , which results in 20%, 40% and 60% degrees of functional

densities). Therefore, the added mass for the degree of organofunctional silanes required (Δm_{silane}) can be calculated as:

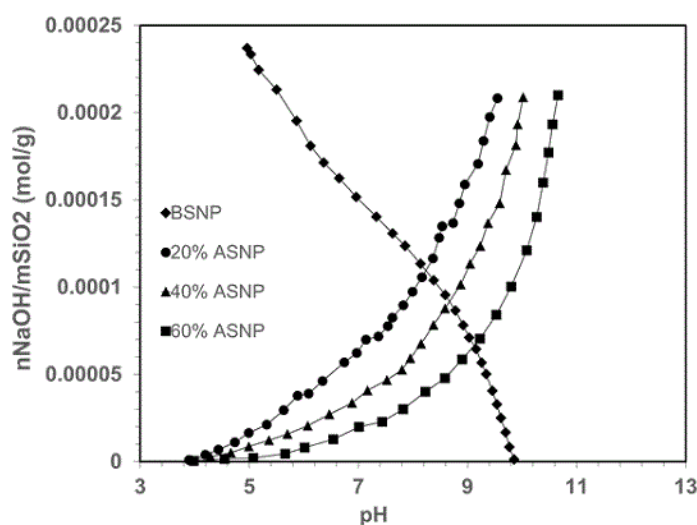
$$\Delta m_{\text{silane}} = n_{\text{silane}} \times M_i$$

And lastly, the volume of organofunctional silanes needed is:

$$\Delta V_{\text{silane}} [\text{ml}] = \Delta m_{\text{silane}} / \rho_{\text{silane}}$$

Supplementary Note 2: Acid-Base titrations and calculations on the functionalized particles

Acid base titrations are used to characterize the efficiency of the silanization reactions performed on the acrylate functionalized silica nanoparticles (ASNPs) functionalized at 20%, 40% and 60% acrylate densities. The curves are derived from the addition of molar concentrations of NaOH and HCl for acrylate and bare silica nanoparticles respectively, which alters the pH of the titration solutions.



Supplementary Figure 2: Acid base titrations on silica nanoparticles. Addition of molar concentrations of hydroxyl ions (OH^-) results in the alteration of the pH of dispersed acrylate functionalized silica nanoparticles, tagged 20%-ASNP, 40%-ASNP and 60%-ASNP. A stock solution of 1M NaOH is used to titrate the acrylate silica nanoparticles whereas 1M HCl is used for the bare silica nanoparticles.

At a chosen pH interval, α_{100} is designated for the slope on the curve resulting from acid base titrations of bare silica nanoparticles (BSNPs), whereas α_{80} , α_{60} and α_{40} are correspondingly designated for 20%-ASNPs, 40%-ASNPs and 60%-ASNPs respectively. The real densities of adsorbed organofunctional silanes are derived thus wise:

$[1 - \alpha_{80}]$, $[1 - \alpha_{60}]$, and $[1 - \alpha_{40}]$ for each of the acrylate groups, which are used to plot for the *calculated densities* (in Note 1, above) verses real densities $[1 - \alpha_x]$.

Supplementary Note 3: Characterization of STrIPS bijel fibers.

Confocal Laser Scanning Microscopy (CLSM) images obtained from scanning at different depths of STrIPS bijel fibers fabricated with acrylated silica nanoparticles (ASNP). ASNP-bijel fibers are processed to obtain 3D reconstructions and bijel-domain size measurements. To demonstrate this, the CLSM image slices obtained from scanning the 60%-ASNP bijel fiber (in main text, Fig. 2a) are used. Supplementary Figure 3a shows the images of confocal scans at different fiber depths. Bijel domain sizes are determined by measuring the dimensions of bicontinuous channels (at multiple locations) as indicated by white lines in the magnified image at 30 μm depth. The average of domain measurements at chosen fiber depths are used to generate Fig. 2b in main text. Supplementary Fig. 3b shows the 3D reconstructed side and front views of a 60%-ASNP STrIPS bijel fiber segment processed at different depths (Δz_i).

Corresponding binary images at chosen fiber depths are used to derive the scaled oil-to-water volume ratio (in main text, Fig. 2d). Using the “adaptive thresholding” plugin for ImageJ, we convert the 2-dimensional micrographs into binary images, from which the percentage area of

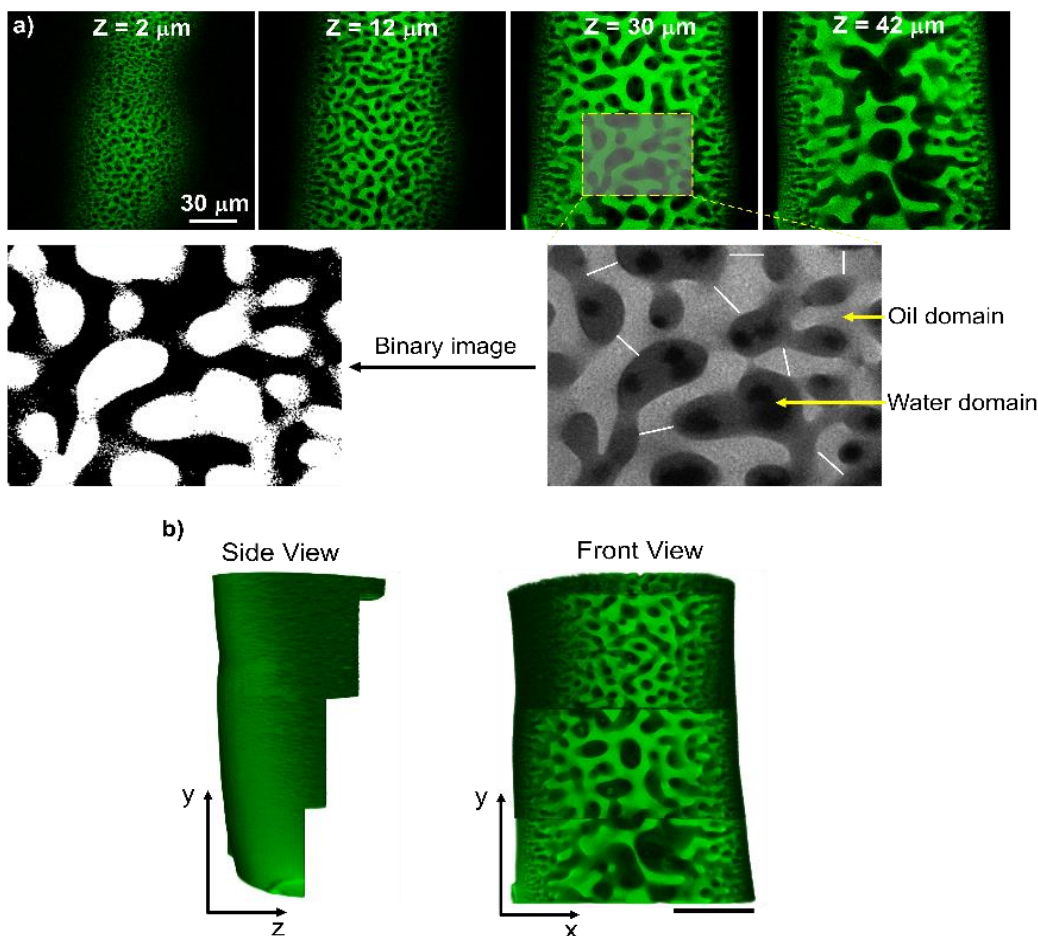
the corresponding oil domains (A_i) are measured at varying depths (Δz_i) of the bijel fiber (supplementary Figure 3b). Hence, the approximated fractional volume of oil (V_o) is calculated as: $A_1\Delta z_1 + A_2\Delta z_2 + A_3\Delta z_3 + \dots\dots A_n\Delta z_n$. The total volume of the bijel (V_T) comprising both oil and water domains is calculated as $A_T(\Delta z_1 + \Delta z_2 + \Delta z_3 + \dots\dots \Delta z_n)$, where A_T is the area of a selected region in chosen confocal slices. Thereby, oil-to-water-volume ratio is derived as V_o/V_T (Figure 2d in main text).

Also, to measure the volume specific surface areas of the ASNP STRIPS bijel fibers (in the main text, Figure 2a), a similar approach for measuring the surface area of previously generated STRIPS bijel fibers, as reported by Haase *et al.*,¹ was used. The volume specific surface area (shown in main text, Figure 2c) is estimated as follows. Sections of the polymerized (BDA) ASNP bijel fibers are subjected to refractive-index matching by first soaking in ethanol and then in pure diethyl phthalate. Following this, a high resolution (1056 X 1056 pixel) confocal image is taken along the equatorial section of the fiber sample. The confocal images are then converted into binary images by using the “adaptive thresholding” plugin from ImageJ. A section of the equatorial binary image is first selected from the center to the surface of the fiber (~20um). The selected section is then segmented into thin strips of Δr . For each stripe region of fiber length (L), the area fraction of oil (A_o) and the perimeter of the curved interfaces ($p(r)$) are determined. Based on the approximation that the bijel fibers have radially uniform internal structures, we estimate the interfacial areas ($A(r)$) and volumes ($V(r)$) of the polymerized bicontinuous scaffold within a thin cylindrical shell as follows:

$$A(r) = 2\pi r.p(r) \text{ and } V(r) = 2\pi rL.A_o.$$

The volume specific surface areas (A_s [$\mu\text{m}^2/\mu\text{m}^3$]) of the bijel fibers (shown in main text, Figure 2c) are calculated as follows:

$$A_s = \frac{\sum_{r=0}^R A(r)}{\sum_{r=0}^R V(r)}$$

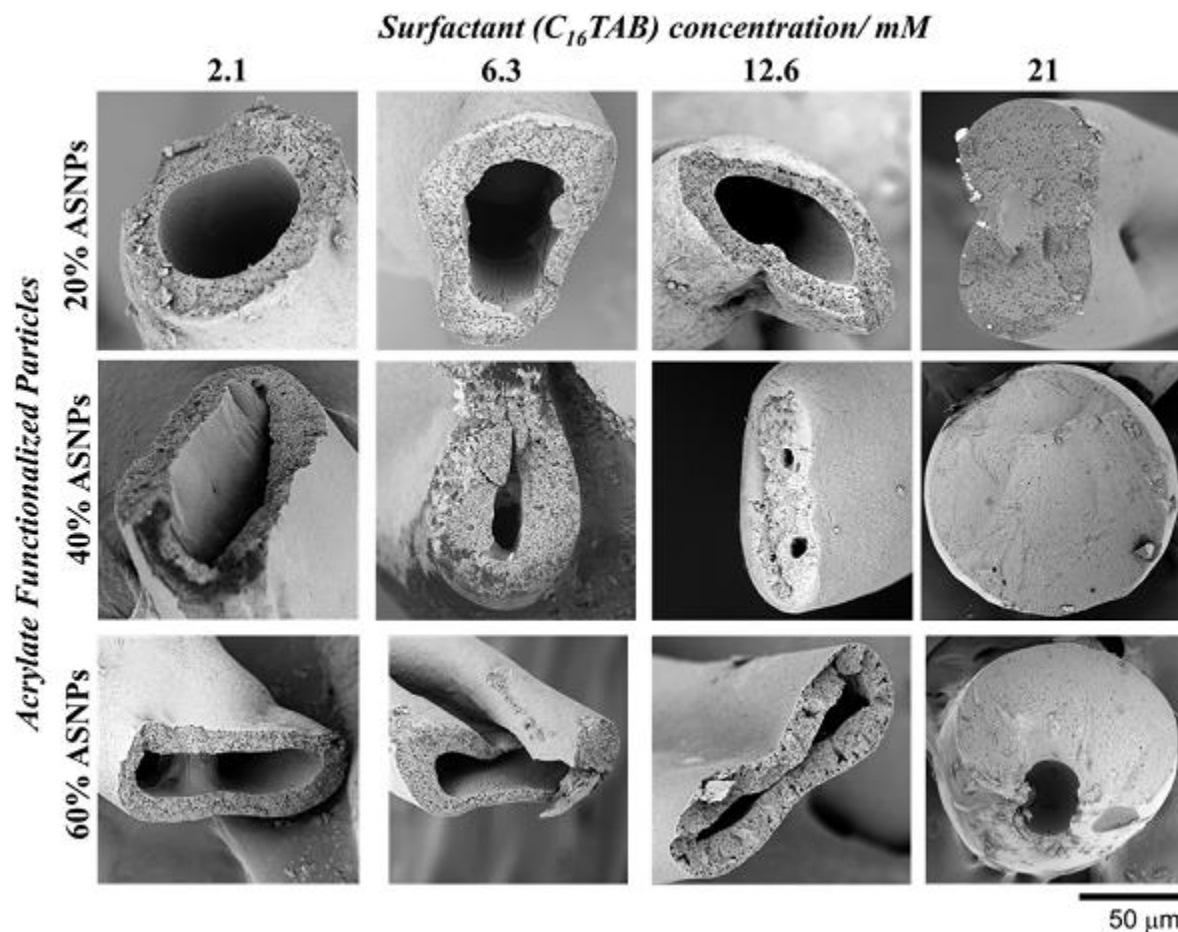


Supplementary Figure 3: Characterization of bijel fibers. a) Confocal laser scanning micrographs of a 60%-ASNP bijel fiber at different depths, where the oil domains are colored as green. To characterize the images, the magnified section (in gray-scale) at for example, $\sim 30 \mu\text{m}$ fiber depth, is converted into a binary image and used to derive the domain size measurements in Fig. 2b (in main text). b) 3D confocal reconstructions of a cascading bijel fiber showing different views, as a result of processing confocal stacks in a stepwise fashion at different depths (Δz_i). This post-processing technique is used to visualize the internal morphologies of STRIPS bijel fibers generated in Figures 2 and 4 (in main text).

Supplementary Note 4: Nucleated STrIPS fibers formed by addition of C₁₆TAB to the ternary mixtures

STrIPS bijel fibers fabricated with ternary mixtures prepared with the surfactant, C₁₆TAB, shows nucleated structures (supplementary Figure 4). Failure to form bicontinuous structures is attributed to the extreme hydrophobicity imparted to the acrylate particles, which likely partitions predominantly into the oil-rich phase, after interacting with long-chain C₁₆TAB surfactants. This also contributes significantly to the hollowness of bijel fibers, as similar to previously observed results,² but are curtailed with the use of a shorter hydrocarbon chain length surfactant (C₁₂TAB), as shown in the main text (Figure 4). Jamming of particles at the surface of the bijel fiber obstructs the transfer of solvent out of the bijel fiber, and in cases where extensive nanoparticle aggregation occurs at the bijel surface, this phenomenon is even more pronounced. We believe that this results in the “trapping” of a water-rich phase inside the bijel fibers, hence the hollowness. Also, it is likely that at high surfactant concentrations, phase inversion occurs leading the formation of an oil-in-water system, for example, at 21mM for 20% ASNPs and 12.6mM and 21mM for 40% ASNPs. Even more interesting is the formation of multiple droplets (water-in-oil-in-water emulsions) at high C₁₆TAB concentrations (21 mM) for 60% ASNPs.

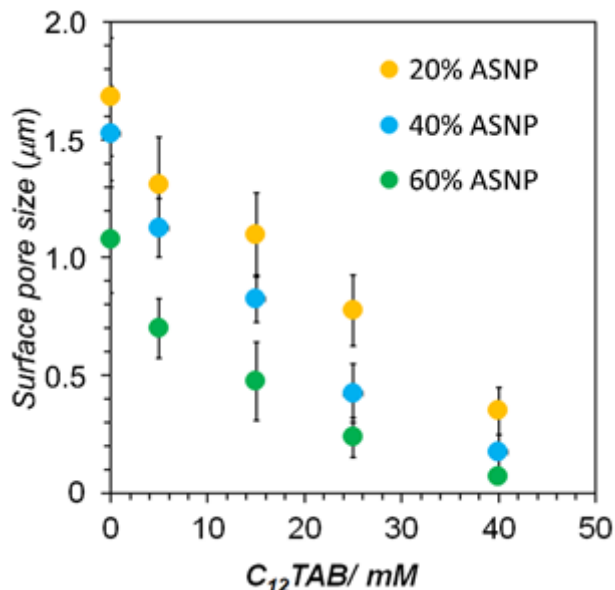
Hence, the absence of interfacial arrest at the internal regions of the bijel fibers - where the water component primarily partitions to – results in hollow fibers. Though undesired, this could be a novel route to fabricate non-bore-fluid bijel hollow-fiber membranes.



Supplementary Figure 4: Scanning Electron Micrographs (SEM) of the resulting structures formed by the direct addition of $C_{16}TAB$ to the ternary mixtures prepared with acrylate silica nanoparticles. In the SEM, the oil domains are polymerized (indicated as gray), whereas the water domains are non-polymerized and subsequently dried up (indicated as dark). The cross sections of the fibers show the presence of nucleated water in oil droplets. At very high surfactant concentrations, fibers fail to form. Instead, oil in water droplets are formed (as observed for the 21 mM $C_{16}TAB$ column), and even further, water-in-oil-in-water droplets are formed for the high acrylate density (60%-ASNPs).

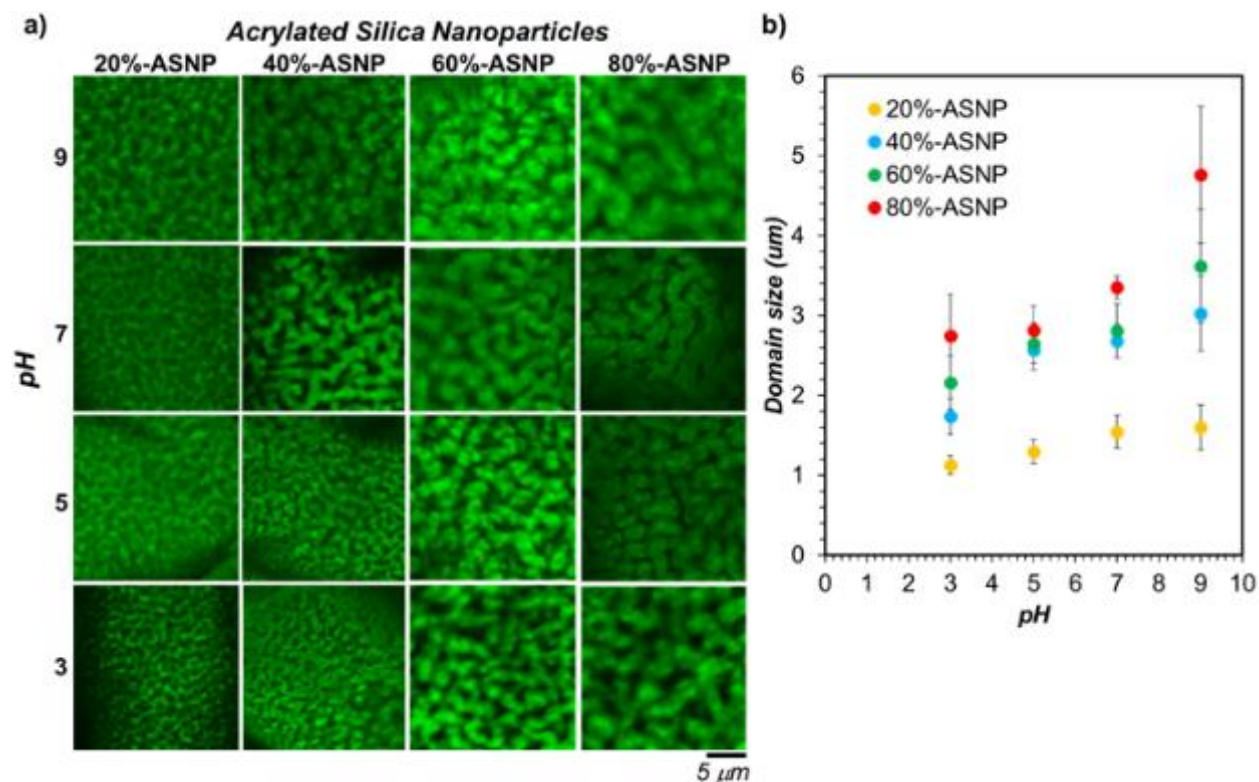
Supplementary Note 5: Surface pore and Domain size characterization of ASNP-STrIPs bijels

In the previous reports of STrIPs bijels where bare silica nanoparticles interacting with C₁₆TAB was used to fabricate bijel fibers, surface pore sizes ranging about 1 μm to 5 μm was measured where it was observed that surface pore sizes decreased with increasing surfactant concentration.^{2,3} In this report where acrylate particles were used, not only does the surface pore sizes decrease with an increase in surfactant (C₁₂TAB) concentration, but also with an increase in the density of acrylate groups. It is however worth noting that the surface pores of ASNP-bijels are relatively smaller (< 2 μm) (see supplementary Figure 5) compared to previous reports,^{2,3} because of the extensive aggregation of hydrophobic acrylate particles at the bijel surface.



Supplementary Figure 5: ASNP-STrIPS bijel fiber surface pore characterization in dependence of surfactant (C₁₂TAB) concentration. The surface pore sizes of ASNP bijel fibers decrease with an increase in surfactant concentration, as well as with the degree of particle acrylation.

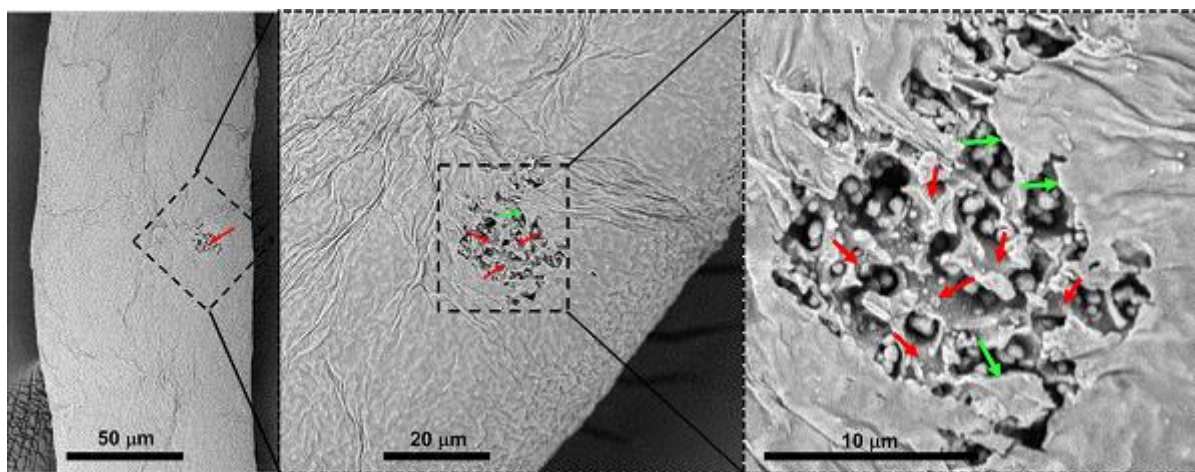
Moreover, we observe that the oil domain sizes of the ASNP-STrIPs bijels (measured at the surface) increase with an increase in the degree of acrylation as well as pH (Supplementary Figure 6a). We believe that this is due to the increased partitioning of higher degrees of acrylate particles into the oil domains, hence, their accumulation in the hydrophobic component of the bijel, causing a corresponding increase in domain size. Additionally, the oil domain sizes increase with an increase in pH. This is likely due to the overall increase in the hydrophobicity of acrylate particles as a result of increased adsorption of cationic surfactant (C₁₆TAB) on the increased negative charges on the particle surface.⁴ Hence, the oil-domain sizes increase as observed in Supplementary Figure 6a, which is characterized and also shown in the graphical plot in 6b.



Supplementary Figure 6: Bijel surface domain size characterization of ASNP-STrIPS bijels. a) Confocal laser scanning micrographs of the surface of STrIPS bijels fabricated with varying degrees of acrylate particles (20%-, 40%-, 60%-, and 80%-ASNPs) and at different pH conditions (decreasing from top to bottom). b) Corresponding bijel surface oil domain size characterization of the confocal images in (a).

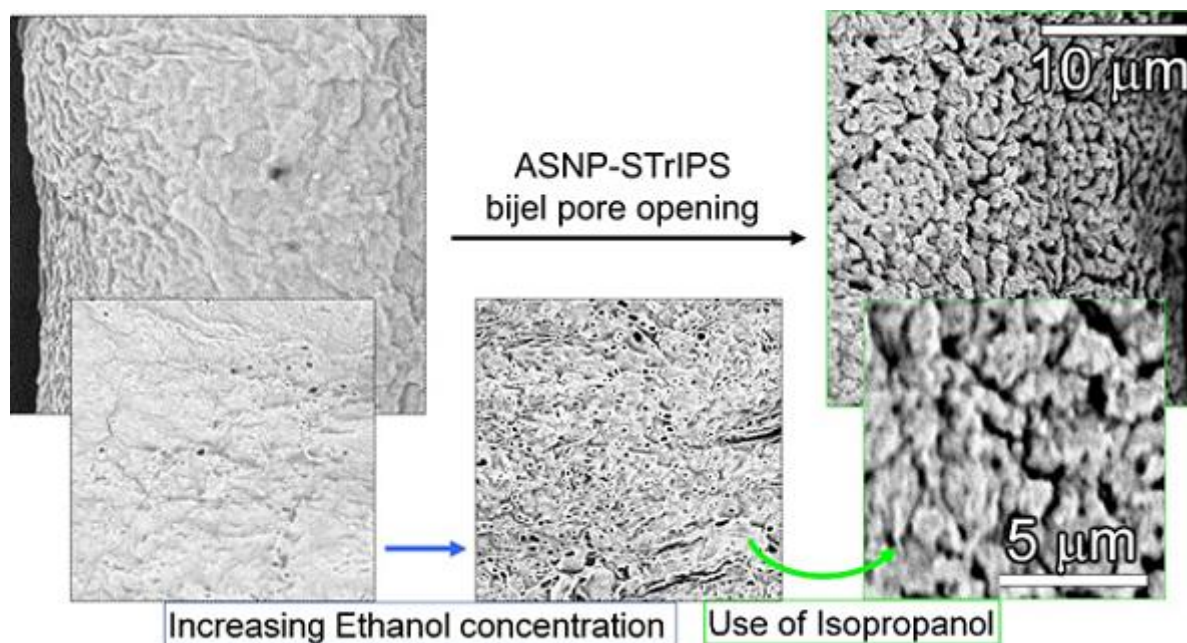
Supplementary Note 6: Control of excess nanoparticles at the surface of ASNP-STrIPS bijels

During STrIPS bijel fabrication, excess nanoparticles aggregate at the surface of the water pores and in effect, covers the underlying bicontinuous structures.^{2,3} Similarly, scanning electron micrographs (SEM) of STrIPS bijels fabricated with acrylated silica nanoparticles show that a thin sheet of aggregated nanoparticles cover the surface of the bijel fiber (Supplementary Figure 7).



Supplementary Figure 7: SEM images of 20%-ASNP STriPS bijel fiber showing the aggregation of nanoparticles at the surface. The red arrow (in the left figure) show an exposed underlying patch of bicontinuous structures which is made more visible in the magnified images (on the right), whereas, the green arrows show the thin film of aggregated nanoparticles on the bijel-fiber surface.

As previously reported, the thin layer of aggregated nanoparticles was partially dispersed when a fraction of ethanol (5 - 20 %) was included in the continuous water phase.³ In our case where hydrophobic acrylate particles were used, even ethanol concentrations of up to 20% v/v was not capable of effectively dispersing the surface-aggregated acrylate particles. Hence, a more apolar solvent, isopropanol (10% v/v) was needed to obtain bijel surface pore opening for ASNP-STriPS bijels (see Supplementary Figure 8).

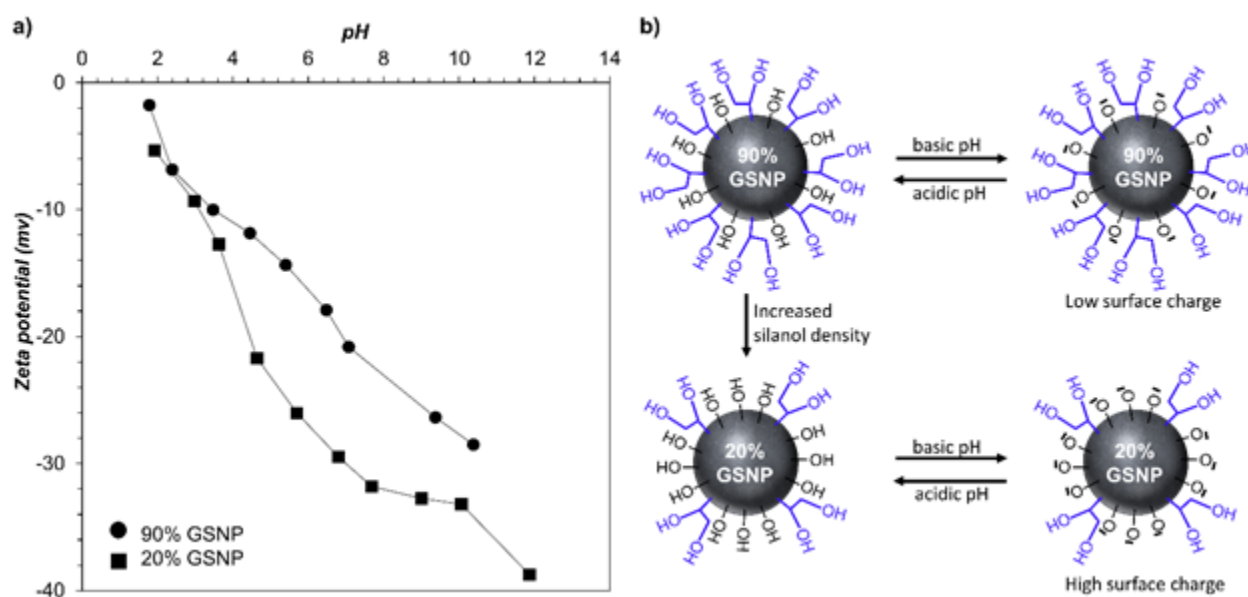


Supplementary Figure 8: Pore size control of ASNP-STrIPS bijel. Effective pore opening is observed when isopropanol (10v/v %), instead of ethanol is used during the fabrication of ASNP-STrIPS bijel fibers. Unlike bare silica nanoparticles, acrylate particles are highly hydrophobic and hence, the surface particle aggregation is more pronounced. The addition of ethanol is not effective in dispersing the aggregated particles. Isopropanol is more effective in dispersing the surface aggregated acrylate particles, resulting in effective surface pore opening.

Supplementary Note 7: Surface Charge Measurements of glycerol functionalized silica nanoparticles particles.

Zeta potential measurements conducted on silica nanoparticles having varying degrees of glycerol functional groups (20% and 90%) show that the density of the functional groups affects the electrophoretic mobility, hence, the measured surface charge. High degrees of functional groups (e.g. 90% glycerol) covering the surface of silica nanoparticles correspond to a low degree of remaining silanol groups (~10% Si-OH), and vice versa. Supplementary Figure 9a shows the zeta potential measurements on silica nanoparticles covered with 20% and 90% glycerol groups, and in dependence of pH. Comparatively, 20%-GSNPs show an increased response to pH

alterations, reflecting a more pronounced dissociation of a higher fraction of available silanol groups, hence a higher magnitude of measured negative surface charges. On the other hand, 90%-GSNPs have relatively less amount of remaining silanol groups resulting in a relatively lower magnitude of surface charges. (see schematic in supplementary Figure 9b).



Supplementary Figure 9: Surface charge measurements of Glycerol functionalized particles. **(a)** Results of zeta potential measurements of 2wt % aqueous dispersions of glycerol functionalized silica nanoparticles (20% and 90% -GSNPs) at different conditions of pH. For a characteristic pH variation (for example, from 3 to 8), the change in magnitude of zeta potential values measured for 20%-GSNPs is relatively higher (~ 22 mV), as compared to a lower magnitude change (~ 13 mV) measured for 90%-GSNPs. This is attributed to the lesser density of remaining silanol groups available for charge dissociation in the case where the functional group density is high. **(b)** Schematic depiction glycerol functionalized silica nanoparticles and their response to pH. At the same basic pH for both 20% and 90% GSNPs, a greater number of negative surface charges are measured for the lesser degree of functional groups.

Supplementary Note 8: Effect of glycerol density and surfactant concentration on STRIPS bijel formation.

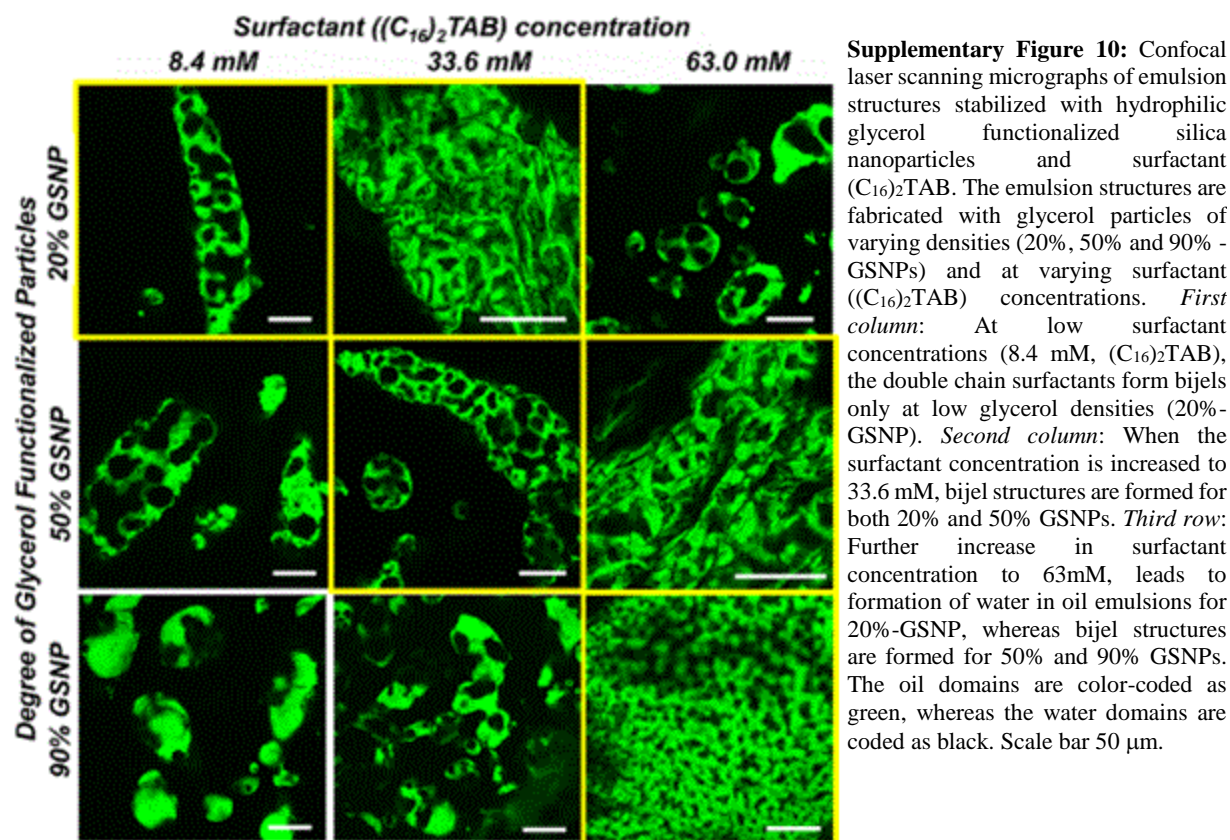
The hydrophilic property of glycerol functionalized particles is expected to increase in relation to an increase in the degree of glycerol groups covering the surface of the silica nanoparticles. The

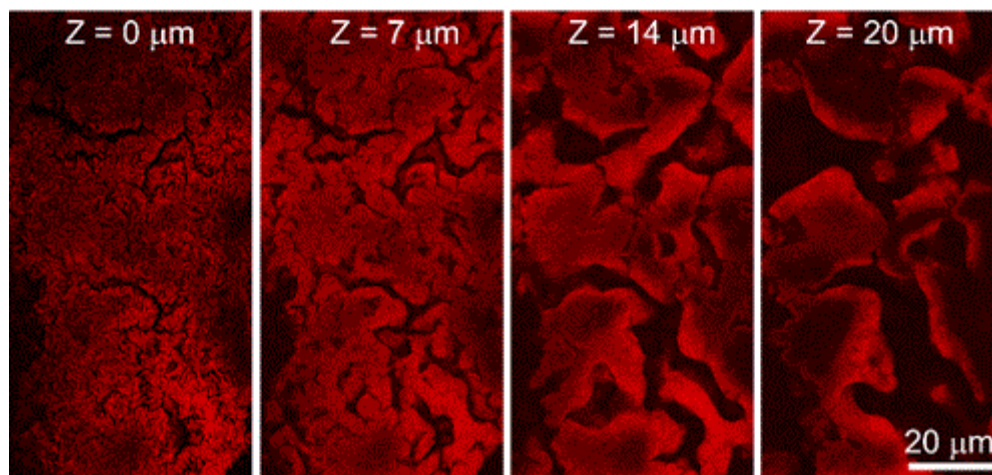
abundance of hydroxyl groups on higher degrees of glycerol (e.g. 90%-GSNP) requires the use of higher concentrations (63 mM) of the cationic surfactant, dihexadecyldimethylammonium bromide ($((C_{16})_2TAB)$) in order to stabilize bijels (see Supplementary Figure 10). Such high surfactant concentrations are required to counter the extreme hydrophilic effect imparted by the high glycerol density. On the other hand, when a similar surfactant concentration (63mM, $(C_{16})_2TAB$) is used on 20%-GSNP, bijels fail to form. Instead, water-in-oil emulsion droplets are formed, depicting particles that have been extensively hydrophobized by the surfactant adsorption. However, the stabilization of viscoelastic structures in the same, depicts the presence of interfacially jammed particles. In effect, a relatively less surfactant concentration (8.4 mM, $(C_{16})_2TAB$) is enough to stabilize bijels made with 20%-GSNPs. For the 50%-GSNPs, it wasn't until surfactant ($((C_{16})_2TAB)$) concentrations reached 12.6 mM that bijel-like structures formed (see

Fig. 5 in main text). Further increase in surfactant concentrations up to 63 mM still resulted in bijel structures (Supplementary Figure 10).

Supplementary Note 9: Dye adsorption on crosslinked bijel scaffolds after fluid remixing

The crosslinked silica nanoparticles scaffold remaining after fluid remixing is visualized under confocal microscopy by rendering the silica particles fluorescent. To realize this, we first increase the pH of the nanoparticle scaffold to generate negative charges on their surface. Subsequently, positively charged Rhodamine (110) dye is introduced to render the crosslinked particles fluorescent, which enable us to visualize the remaining scaffold under confocal microscopy (Supplementary Figure 11).





Supplementary Figure 11: Confocal Laser Scanning Micrographs of fluorescent crosslinked STRIPS bijels after fluid remixing. To cause fluid remixing in the crosslinked bijel, ethanol is added which removes both fluids (oil and water) from the bicontinuous domains, but the nanoparticle crosslinked scaffold remains (Figure 6d). Water is then added multiple times to dilute the ethanol and also to introduce scaffold to an aqueous bath for pH adjustments. A basic buffer solution (1 M NaH_2PO_4) is introduced to the aqueous bath to adjust the pH to 12, which leads to the dissociation of the remaining silanol groups on the surface of the crosslinked glycerol silica nanoparticles. Excess basic water is removed by washing with DI water multiple times, after which the positively charged Rhodamine (110) dye is introduced. Prior to the addition of the dye, the entire crosslinked bijel scaffold remains dark under the confocal microscope is made visible when the dye adsorbs onto the silica particle scaffold. The bijel scaffold deflated upon fluid remixing, hence the observed shifting the equatorial axis (from $\sim 40 \mu\text{m}$ to $20 \mu\text{m}$).

References

- 1 E. F. Vansant, P. Van Der Voort and K. C. Vrancken, *Characterization and chemical modification of the silica surface*, Elsevier, 1995, vol. 93.
- 2 M. F. Haase, K. J. Stebe and D. Lee, *Advanced Materials*, 2015, **27**, 7065–7071.
- 3 M. F. Haase, H. Jeon, N. Hough, J. H. Kim, K. J. Stebe and D. Lee, *Nature Communications*, 2017, **8**, 1234.
- 4 T. G. Anjali and M. G. Basavaraj, *Langmuir*, 2018, **34**, 13312–13321.